

Characterizing planetary orbits and the trajectories of light in the Schwarzschild metric

F. T. Hioe* and David Kuebel

*Department of Physics, St. John Fisher College, Rochester, New York 14618
and Department of Physics & Astronomy, USA University of Rochester, Rochester, New York 14627, USA
(Received 5 January 2010; published 9 April 2010)*

Exact analytic expressions for planetary orbits and light trajectories in the Schwarzschild geometry are presented. A new parameter space is used to characterize all possible planetary orbits. Different regions in this parameter space can be associated with different characteristics of the orbits. The boundaries for these regions are clearly defined. Observational data can be directly associated with points in the regions. A possible extension of these considerations with an additional parameter for the case of Kerr geometry is briefly discussed.

DOI: 10.1103/PhysRevD.81.084017

PACS numbers: 04.20.Jb, 02.90.+p

I. INTRODUCTION

Nearly a century after Einstein's theory of general relativity was found to correctly predict the precession of the planet Mercury around the Sun and the deflection of light by the Sun's gravitational field, the problem of understanding orbital trajectories around very massive objects still retains interest as it relates to current astrophysical topics [1] such as the study of gravitational waves. Among the numerous works on this subject, we should mention the classic publications of Whittaker [2], Hagihara [3] and Chandrasekhar [4] on the Schwarzschild geometry, and the more recent work of Levin and Perez-Giz [5] on the Schwarzschild and Kerr geometries.

In the work of Chandrasekhar and that of Hagihara, the orbits are classified into various types according to the roots of a certain cubic equation, while in the work of Levin and Perez-Giz, the orbits are classified topologically by a triplet of numbers that indicate the numbers of zooms, whirls, and vertices. In the work of Levin and Perez-Giz, the orbits were obtained by numerically integrating the integrable equations. These authors used the planet's energy and angular momentum as the principal physical parameters, and made extensive use of an effective potential for describing the Schwarzschild orbits, as most studies on the topics of general relativity do.

In this paper, we first present, in Sec. II, three explicit analytic expressions for the orbits in the Schwarzschild geometry: one is for periodic [6] and unbounded orbits, and two are terminating orbits. The explicit analytic expressions that we derive not only describe the precise features of the orbits (periodic, precessing, nonperiodic, terminating, etc.) but also clearly indicate two physical parameters which can be used to characterize these orbits. These two dimensionless parameters are specific combinations of the following physical quantities: the total energy and angular momentum of the planet, the masses of the massive object and the planet, and, of course, the universal gravitation

constant G and the speed of light c . These two physical dimensionless parameters were first used by one of us in Ref. [6]. We shall refer to these two quantities as the energy eccentricity parameter e and the gravitational field parameter s , respectively, (or simply as the energy parameter and the field parameter). They will be defined in Sec. II. We will use neither the common convention of setting $G = c = 1$, nor the energy and angular momentum of the planet by themselves, as the physical parameters for characterizing the orbits. With the energy parameter ($0 \leq e \leq \infty$) plotted on the horizontal axis and the field parameter ($0 \leq s \leq \infty$) plotted on the vertical axis, the parameter space for all possible orbits will be shown to be divisible into three sectors, which we call Regions I, II, and II', that have clearly defined boundaries. Region I permits periodic, unbounded, and terminating orbits. Regions II and II' permit terminating orbits only.

In Sec. III, we describe Region I (for $0 \leq e \leq 1$) and the orbits in greater detail. We first divide Region I by lines each of which represents orbits described by elliptic functions of the same modulus k . We then give a more physical division of Region I, which consists of nearly horizontal lines each of which represents orbits that have the same precession angle $\Delta\phi$, and of bent vertical lines each of which represents orbits that have the same "true" eccentricity ε . The terminating orbits will be characterized by two parameters one of which is the angle at which the planet enters the center of the black hole, and the other being the initial distance of the planet from the star or black hole. In Sec. IV, we describe Regions II and II' (for $0 \leq e \leq 1$) in which all orbits are terminating, and we again divide Region II by curves of constant modulus k each of which describes orbits with the same modulus. Regions II and II' are separated by the Schwarzschild horizon. In Sec. V, we describe orbits corresponding to $e > 1$ for Regions I and II. Our "map" in the parameter space (e, s) thus describes all possible orbits in the Schwarzschild geometry in their entirety. The observational data related to a planet's orbit about some giant star or black hole can be directly identified with a point having

*fhioe@sjfc.edu

certain coordinates (e, s) on our map, which can then be used for estimating the physical characteristics associated with the star or black hole and that of the planet itself, assuming that the star or black hole is not spinning very fast. For the Kerr geometry, another dimensionless quantity, which is clearly the ratio of the spin angular momentum per unit mass of the black hole to the orbital angular momentum per unit mass of the planet, should enter into the consideration. In Sec. VI, we briefly discuss a possible extension of our results to the case involving a slowly spinning black hole, at least to the first order perturbation, by rescaling the physical parameters involved.

In Sec. VII, we study the deflection of light by the gravitational field of a very massive object. A single dimensionless parameter will be used to characterize the region. We show that here too, we should divide the region into three sectors, which we again call Regions I, II, and II', and we present three analytic expressions for the trajectories of light applicable in these different regions. Region I has trajectories of light that get deflected, and Regions II and II' have trajectories of light that are absorbed by and terminate at the black hole.

In Sec. VIII, we give a summary of our results. Proof of many interesting analytic relations among the parameters appearing in these studies are given in several appendices. Since our results presented in this paper cover gravitational fields of all ranges, from the weak field produced by the Sun of our Solar System, for example, to the very strong field produced by a black hole, we want to avoid referring to the massive object that produces the gravitational field as a black hole, and prefer to refer to it as the star or black hole, and we shall refer to the object of a much smaller mass that orbits around it as the planet or the particle.

We have supplemented our many analytic results with numerous tables that present various physical quantities such as the minimum and maximum distances of the planet from the star and the angles of precession of the orbits that are calculated from our analytic expressions, as well as numerous figures that show various kinds of orbits of the planet and various kinds of deflection of light.

II. ANALYTIC EXPRESSIONS FOR THE ORBITS

We consider the Schwarzschild geometry, i.e. the static spherically symmetric gravitational field in the empty space surrounding some massive spherical object such as a star or a black hole of mass M . The Schwarzschild metric for the empty spacetime outside a spherical body in the spherical coordinates r, θ, ϕ is [1]

$$dl^2 = c^2 \left(1 - \frac{\alpha}{r}\right) dt^2 - \left(1 - \frac{\alpha}{r}\right)^{-1} dr^2 - r^2 d\theta^2 - r^2 \sin^2 \theta d\phi^2, \quad (1)$$

where

$$\alpha = \frac{2GM}{c^2} \quad (2)$$

is known as the Schwarzschild radius, G is the universal gravitation constant, and c is the speed of light. If $[x^\mu] = (t, r, \theta, \phi)$, then the worldline $x^\mu(\tau)$, where τ is the proper time along the path, of a particle moving in the equatorial plane $\theta = \pi/2$, satisfies the equations [1]

$$\left(1 - \frac{\alpha}{r}\right) \dot{t} = \kappa, \quad (3)$$

$$c^2 \left(1 - \frac{\alpha}{r}\right) \dot{t}^2 - \left(1 - \frac{\alpha}{r}\right)^{-1} \dot{r}^2 - r^2 \dot{\phi}^2 = c^2, \quad (4)$$

$$r^2 \dot{\phi} = h, \quad (5)$$

where the derivative $\dot{}$ represents $d/d\tau$. The constant h is identified as the angular momentum per unit mass of the planet, and the constant κ is identified to be

$$\kappa = \frac{E}{m_0 c^2},$$

where E is the total energy of the planet in its orbit and m_0 is the rest mass of the planet at $r = \infty$. Substituting Eqs. (3) and (5) into (4) gives the ‘‘combined’’ energy equation [1]

$$\dot{r}^2 + \frac{h^2}{r^2} \left(1 - \frac{\alpha}{r}\right) - \frac{c^2 \alpha}{r} = c^2 (\kappa^2 - 1). \quad (6)$$

Substituting $dr/d\tau = (dr/d\phi)(d\phi/d\tau) = (h/r^2) \times (dr/d\phi)$ into the combined energy equation gives the differential equation for the orbit of the planet

$$\left(\frac{du}{d\phi}\right)^2 = \alpha u^3 - u^2 + Bu + C, \quad (7)$$

where $u = 1/r$, $B = 2GM/h^2$, $C = c^2(\kappa^2 - 1)/h^2$. Following Whittaker [2], it is convenient to change variable from u to a dimensionless quantity U defined by

$$U = \frac{1}{4} \left(\frac{\alpha}{r} - \frac{1}{3}\right) = \frac{1}{4} \left(\alpha u - \frac{1}{3}\right), \quad (8)$$

or $u = 4U/\alpha + 1/(3\alpha)$ so that Eq. (7) becomes

$$\left(\frac{dU}{d\phi}\right)^2 = 4U^3 - g_2 U - g_3, \quad (9)$$

where

$$g_2 = \frac{1}{12} - s^2 \quad g_3 = \frac{1}{216} - \frac{1}{12}s^2 + \frac{1}{4}(1 - e^2)s^4, \quad (10)$$

and where

$$e = \left[1 + \frac{h^2 c^2 (\kappa^2 - 1)}{(GM)^2}\right]^{1/2}, \quad (11)$$

and

$$s = \frac{GM}{hc}. \quad (12)$$

The two dimensionless parameters e and s , which are defined by the two above equations and which we call the energy and field parameters, respectively, will be the principal parameters we shall use for characterizing the orbit of a planet. It will be noted that the constant $c^2(\kappa^2 - 1)$, which is <0 for a bound orbit, can be identified with $2E_0/m$ in the Newtonian limit, where E_0 is the sum of the kinetic and potential energies and is <0 for a bound orbit, and is ≥ 0 for an unbound orbit, and m is the mass of the planet (which approaches m_0), and that

$$e \simeq \left[1 + \frac{2E_0 h^2}{m(GM)^2} \right]^{1/2} \quad (13)$$

is the ‘‘eccentricity’’ of the orbit. Also, in the small s limit, the orbit equation can be shown to be given by

$$\frac{1}{r} \simeq \frac{GM}{h^2} [1 - e \cos(1 - \delta)\phi], \quad (14)$$

where $\delta \simeq 3(GM)^2/(hc)^2$. Thus, r assumes the same value when ϕ increases to $\phi + 2\pi/(1 - \delta)$. Comparing this with the increase of ϕ from ϕ to $\phi + 2\pi$, the ellipse will rotate about the focus by an amount which is the angle of precession

$$\Delta\phi \simeq \frac{2\pi}{1 - \delta} - 2\pi \simeq 2\pi\delta = \frac{6\pi(GM)^2}{h^2 c^2}. \quad (15)$$

This is the well-known approximate expression for the precession angle for the case of very small s . The limiting case for $\delta = 0$ is the well-known orbit equation in Newtonian mechanics. We should note that while the limit $s = 0$ (and thus $\delta = 0$) cannot be strictly correct in principle so long as $M \neq 0$, this limit can be used for many practical cases with great accuracy as evidenced by the predictions of Newtonian mechanics. A special case of these Newtonian orbits is the circular orbit of radius $r = h^2/GM$ for $e = 0$.

We now derive the exact analytic solutions of Eq. (9) and classify the three possible solutions from a purely mathematical viewpoint, and we shall consider their physical interpretations in the next section. We first define the discriminant Δ of the cubic equation

$$4U^3 - g_2U - g_3 = 0, \quad (16)$$

by

$$\Delta = 27g_3^2 - g_2^3. \quad (17)$$

The three roots of the cubic Eq. (16) are all real for the case $\Delta \leq 0$. We call the three roots e_1, e_2, e_3 and arrange them so that $e_1 > e_2 > e_3$; the special cases when two of the roots are equal will be considered also. For the case $\Delta > 0$, the cubic Eq. (16) has one real root and two roots that are complex conjugates. The analytic solutions of Eq. (9) that we shall present will give the distance r of the planet from the star or black hole in terms of the Jacobian elliptic functions that have the polar angle ϕ in

their argument and that are associated with a modulus k that will be defined. Instead of writing r , we use the dimensionless distance q measured in units of the Schwarzschild radius α and defined by

$$q \equiv \frac{r}{\alpha} \equiv \frac{1}{\alpha u}. \quad (18)$$

The dimensionless distance q is related to U of Eq. (8) by

$$\frac{1}{q} = \frac{1}{3} + 4U. \quad (19)$$

We now give the three analytic solutions of Eq. (9) in the following.

Solution (A1) For $\Delta \leq 0$, $e_1 > e_2 \geq U > e_3$.

Writing the right-hand side of Eq. (9) as $4(e_1 - U)(e_2 - U)(U - e_3)$, Eq. (9) can be integrated with ϕ expressed in terms of the inverse Jacobian sn function [7]. After a little algebra and some rearrangement, the equation for the orbit is found to be

$$\begin{aligned} \frac{1}{q} &= \frac{1}{3} + 4e_3 + 4(e_2 - e_3)sn^2(\gamma\phi, k) \\ &= \frac{1}{3} + 4e_3 + 4(e_2 - e_3) \frac{1 - cn(2\gamma\phi, k)}{1 + dn(2\gamma\phi, k)}, \end{aligned} \quad (20)$$

where the point at $\phi = 0$ has been chosen to give $U = e_3$. The constant γ appearing in the argument, and the modulus k , of the Jacobian elliptic functions are given in terms of the three roots of the cubic Eq. (16) by

$$\gamma = (e_1 - e_3)^{1/2}, \quad (21)$$

$$k^2 = \frac{e_2 - e_3}{e_1 - e_3}, \quad (22)$$

where e_1, e_2, e_3 are given by

$$\begin{aligned} e_1 &= 2\left(\frac{g_2}{12}\right)^{1/2} \cos\left(\frac{\theta}{3}\right), & e_2 &= 2\left(\frac{g_2}{12}\right)^{1/2} \cos\left(\frac{\theta}{3} + \frac{4\pi}{3}\right), \\ e_3 &= 2\left(\frac{g_2}{12}\right)^{1/2} \cos\left(\frac{\theta}{3} + \frac{2\pi}{3}\right), \end{aligned} \quad (23)$$

and where

$$\cos\theta = g_3 \left(\frac{27}{g_2^3}\right)^{1/2}. \quad (24)$$

Equation (20) is valid for orbits for all values of e but for restricted values of s , as will be shown. It was first given in Ref. [6] using a slightly different approach that was initiated by Whittaker [2] for describing the precessional orbits for $0 \leq e < 1$. It was shown to reduce to Eq. (14) for the case of very small s , which in turn gave the known approximate precession angle given by Eq. (15). The modulus k of the elliptic functions has a range $0 \leq k^2 \leq 1$. For the special case of $k^2 = 1$, $sn(\gamma\phi, 1) = \tanh(\gamma\phi)$, $cn(\gamma\phi, 1) = dn(\gamma\phi, 1) = \text{sech}(\gamma\phi)$, and we shall refer to

the orbit given by Eq. (20) as the asymptotic elliptic-, parabolic-, or hyperbolic-type orbit for $0 \leq e < 1$, $e = 1$, or $e > 1$.

The period of $cn(2\gamma\phi, k)$ is $4K(k)$, and the period of $dn(2\gamma\phi, k)$ and of $sn^2(\gamma\phi, k)$ is $2K(k)$, where $K(k)$ is the complete elliptic integral of the first kind [7]. For $k = 0$, $sn(x, 0) = \sin x$, $cn(x, 0) = \cos x$, $dn(x, 0) = 1$. As k^2 increases from 0 to 1, $K(k)$ increases from $\pi/2$ to ∞ . For an elliptic-type orbit, the distance r of the planet from the center of the star or black hole assumes the same value when its polar angle ϕ increases from ϕ to $\phi + 4K/(2\gamma) = \phi + 2K/\gamma$. Comparing this with the increase of ϕ from ϕ to $\phi + 2\pi$ in one revolution, the perihelion (or the aphelion) will rotate by an amount

$$\Delta\phi = \frac{2K(k)}{\gamma} - 2\pi, \quad (25)$$

which is the exact expression for the precession angle. For k^2 close to the value 1, the planet can make many revolutions around the star or black hole before assuming a distance equal to its initial distance. Thus, if n is the largest integer for which $2K(k)/\gamma$ is equal to or greater than $2n\pi$, the angle of precession should be more appropriately defined as $2K(k)/\gamma - 2n\pi$. For the sake of consistency, however, we shall stick to the definition given by Eq. (25).

For the case of very small s and to the order of s^2 , it was shown in Ref. [6] that $e_1 \simeq 1/6 - s^2$, $e_2 \simeq -1/12 + (1 + e)s^2/2$, $e_3 \simeq -1/12 + (1 - e)s^2/2$, $\theta \simeq 2\sqrt{27}es^2$, $\gamma \simeq [1 - (3 - e)s^2]/2$, $k^2 \simeq 4es^2$, $K(k) \simeq \pi(1 + es^2)/2$, and substituting these into Eq. (25) gives the well-known approximate result given by Eq. (15).

For the periodic orbits, we note that the maximum distance r_{\max} (the aphelion) of the planet from the star or black hole and the minimum distance r_{\min} (the perihelion) of the planet from the star or black hole, or their corresponding dimensionless forms q_{\max} ($= r_{\max}/\alpha$) and q_{\min} ($= r_{\min}/\alpha$), are obtained from Eq. (20) when $\gamma\phi = 0$ and when $\gamma\phi = K(k)$, respectively, and they are given by

$$\frac{1}{q_{\max}} = \frac{1}{3} + 4e_3, \quad (26)$$

and

$$\frac{1}{q_{\min}} = \frac{1}{3} + 4e_2, \quad (27)$$

where e_2 and e_3 are determined from Eqs. (23), (24), and (10) in terms of e and s .

Although we may call the orbits given by this solution for $0 \leq k^2 < 1$ and $0 \leq e < 1$ periodic, they are not necessarily closed orbits. It is seen from the precession discussed above that for $\Delta\phi = f\pi$, unless f is a rational number, the orbit will not close and it is not strictly a closed periodic orbit. However, for all practical purposes, any irrational number when truncated becomes a rational

number, and thus the orbit will be closed. The distinction of closed and nonclosed orbits depending on whether f is rational or irrational is of course of profound theoretical interest [5].

For a general periodic orbit that precesses, the general or true eccentricity ε of the orbit is defined by

$$\varepsilon \equiv \frac{r_{\max} - r_{\min}}{r_{\max} + r_{\min}} = \frac{q_{\max} - q_{\min}}{q_{\max} + q_{\min}}, \quad (28)$$

where q_{\max} and q_{\min} are given by Eqs. (26) and (27).

We shall show in the following section that the true eccentricity ε is in general not equal to the energy eccentricity parameter e defined by Eq. (11), but that $\varepsilon \rightarrow e$ in the limit of $s \rightarrow 0$, i.e. in the Newtonian limit. For the special case of $\varepsilon = 1$, however, we shall show that it coincides with the special case of $e = 1$ for all applicable values of s , and that it signifies an unbounded orbit.

We now proceed to present the second solution.

Solution (A2) For $\Delta \leq 0$, $U > e_1 > e_2 > e_3$.

We write the right-hand side of Eq. (9) as $4(U - e_1) \times (U - e_2)(U - e_3)$ and Eq. (9) can be integrated with ϕ expressed in term of the inverse Jacobian sn function [7]. The equation for the orbit is found to be

$$\frac{1}{q} = \frac{1}{3} + 4 \frac{e_1 - e_2 sn^2(\gamma\phi, k)}{cn^2(\gamma\phi, k)}, \quad (29)$$

where γ , k , e_1 , e_2 , and e_3 are given by Eqs. (21)–(24) as in the first solution. This solution gives a terminating orbit. The point at $\phi = 0$ has been chosen to be given by

$$\frac{1}{q_1} = \frac{1}{3} + 4e_1. \quad (30)$$

The planet, starting from the polar angle $\phi = 0$ at a distance q_1 from the black hole, plunges into the center of the black hole when its polar angle ϕ_1 is given by $cn(\gamma\phi_1, k) = 0$, i.e. when

$$\phi_1 = \frac{K(k)}{\gamma},$$

where γ and k are given by Eqs. (21) and (22).

The region of (e, s) where orbits given by Solutions A1 and A2 are applicable will be called Region I, and it will be described in greater detail in Sec. III. Thus, each point (e, s) of parameter space in Region I represents two distinct orbits, one periodic and one terminating. At the same coordinate point, the characteristic quantities that describe the two distinct orbits are related. For example, by noting $e_1 + e_2 + e_3 = 0$ and from Eqs. (26) and (27), q_1 can be expressed as

$$\frac{1}{q_1} = 1 - \left(\frac{1}{q_{\min}} + \frac{1}{q_{\max}} \right), \quad (31)$$

where q_{\min} and q_{\max} are the minimum and maximum distances for the periodic orbit at the same coordinate points (e, s) . It will be noted that q_1 is less than q_{\min} , i.e.

for the terminating orbit the planet is assumed initially to be closer to the black hole than the q_{\min} for the associated periodic orbit, except at $k^2 = 1$, where $q_1 = q_{\min}$ and the planet has a circular instead of a terminating orbit that will be explained later.

We note that the terminating orbit Eq. (29) presented has no singularity at the Schwarzschild horizon $q = 1$, because, as is well known, $q = 1$ is a coordinate singularity and not a physical singularity. The orbit obtained from continuing ϕ beyond the value $\phi_1 = K(k)/\gamma$ re-emerges from the singularity at $q = 0$. This behavior is perhaps similar to the conjectured trajectory of a particle that is emitted from a so-called “white hole” [1]. The orbit beyond $\phi = \phi_1$ is shown as a dotted line in the figures that show the terminating orbits.

For now, the orbits in Region I are characterized mathematically by $\Delta \leq 0$.

We now present the third solution.

Solution (B) For $\Delta > 0$.

Define

$$A = \frac{1}{2} \left(g_3 + \sqrt{\frac{\Delta}{27}} \right)^{1/3}, \quad B = \frac{1}{2} \left(g_3 - \sqrt{\frac{\Delta}{27}} \right)^{1/3}, \quad (32)$$

where g_3 and Δ are defined by Eqs. (10) and (17). The real root of the cubic Eq. (16) is given by

$$a = A + B, \quad (33)$$

and the two complex conjugate roots b and \bar{b} are $-(A + B)/2 \pm (A - B)\sqrt{3}i/2$. We further define

$$\gamma = [3(A^2 + AB + B^2)]^{1/4} \quad (34)$$

and

$$k^2 = \frac{1}{2} - \frac{3(A + B)}{4\sqrt{3}(A^2 + AB + B^2)} = \frac{1}{2} - \frac{3a}{4\gamma^2}. \quad (35)$$

Writing the right-hand side of Eq. (9), with $U \geq a$, as $4(U - a)(U - b)(U - \bar{b})$, Eq. (9) can be integrated with ϕ expressed in terms of the inverse Jacobian cn function [7]. We find the equation for the orbit to be

$$\begin{aligned} \frac{1}{q} &= \frac{1}{3} + 4a + 4\gamma^2 \frac{1 - cn(2\gamma\phi, k)}{1 + cn(2\gamma\phi, k)} \\ &= \frac{1}{3} + 4a + 4\gamma^2 t^2(\gamma\phi, k) dn^2(\gamma\phi, k). \end{aligned} \quad (36)$$

This is a terminating orbit. The initial distance q_2 of the planet at $\phi = 0$ has been chosen to be given by

$$\frac{1}{q_2} = \frac{1}{3} + 4a. \quad (37)$$

It plunges into the center of the black hole when its polar angle $\phi = \phi_2$ is given by

$$\phi_2 = \frac{K(k)}{\gamma},$$

where γ and k are given by Eqs. (34) and (35). Again, we note that the orbit Eq. (36) has no singularity at $q = 1$.

The region of (e, s) where orbits given by Eq. (36) are applicable will be divided into two sectors called Regions II and II', the boundary between which will be defined later. They have terminating orbits only. For now, the orbits in Regions II and II' are characterized mathematically by $\Delta > 0$.

As for the initial points of the orbits discussed above, by comparing Eq. (19) with the orbit Eqs. (20), (29), and (36), and with Eqs. (26), (30), and (37), we already noted that our choice of $\phi = 0$ in our orbit equations is such that for $0 \leq e \leq 1$ it gives $U = e_3, e_1$, and a , respectively, that in turn give $q = q_{\max}, q_1$, and q_2 as the initial distances of the planet from the star or black hole. We then note from Eq. (9) that $dU/d\phi = 0$ and hence $dr/d\phi = 0$ for the planet at these initial points of the trajectories, i.e. the trajectory or more precisely the tangent to the trajectory at $\phi = 0$ is perpendicular to the line joining the planet to the star or black hole. All this will be seen in the figures presented later, and all our references to the initial position of the planet from here onward, for the case $0 \leq e \leq 1$, assume that the trajectory (as ϕ increases from 0) of the planet at its initial position is perpendicular to the line joining the planet to the star or black hole.

In Secs. III and IV, we shall consider the case $0 \leq e \leq 1$, and we shall discuss the case $e > 1$ in Sec. V.

III. REGION I FOR $0 \leq e \leq 1$

Consider the orbits expressed by Eqs. (20) and (29) given by Solutions A1 and A2 and characterized mathematically by $\Delta \leq 0$. We call the region covered by the associated range of values for (e, s) Region I. In this section, we shall be mainly concerned with the values of e in the range $0 \leq e \leq 1$, and we shall deal with the values of e in the range $e > 1$ in Sec. V.

To gain a preliminary perspective, consider the Earth (as the planet) and the Sun (as the star) in our Solar System. Substituting the mass of the Sun $M = M_S = 1.99 \times 10^{30}$ kg and the angular momentum of the Earth per unit mass of the Earth $h = 4.48 \times 10^{15}$ m²/s, we find $s = 0.983 \times 10^{-4}$. The energy eccentricity parameter e , which is equal to the true eccentricity ε of the Earth's orbit for such a very small s value, is known to be about 0.017. The approximate relation $k^2 \simeq 4es^2$ gives the squared modulus of the elliptic functions that describe the Earth's orbit to be $k^2 = 0.657 \times 10^{-9}$. We see that for the planetary system that is familiar to us, the values of s and k^2 are very small indeed. We may also note that the Schwarzschild radius $\alpha = 2GM_S/c^2 \simeq 3$ km would be well inside the Sun which has a radius of 6.96×10^5 km. The Earth's dimensionless distance is $q \simeq 5 \times 10^7$ from the Sun's center. For this value of s , with $q_{\min} \simeq q_{\max} \simeq 5 \times 10^7$, the orbit given by Eq. (29) from Solution (A2) would require the initial position q_1 of a planet to be $\simeq 1$ according to Eq. (31), i.e.

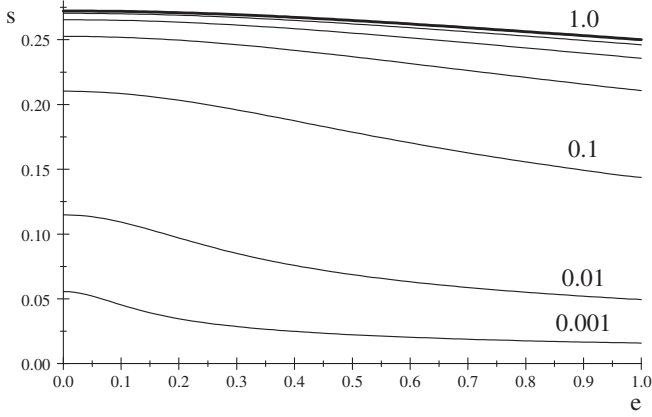


FIG. 1. Region I plots of $k^2 = 0.001, 0.01, 0.1, 0.3, 0.5, 0.7, 1.0$.

the planet would have to be at a distance equal to the Schwarzschild radius from the center of the Sun for it to have a terminating orbit which plunges to the center of the Sun. Therefore, the terminating orbit given by Eq. (29) is inapplicable for our Solar System. The periodic and unbounded orbits, on the other hand, are perfectly valid.

However, for cases when the massive object is a gigantic mass concentrated in a small radius such as a black hole, all the possibilities presented here may arise. As the field parameter s increases from 0, the modulus k of the elliptic functions that describe the planet's orbits also increases. From Eqs. (21)–(24), it is seen that several steps are needed to relate k^2 to e and s . In Appendix A, we show that a direct relationship between k^2 and e and s can be established, and it is given by

$$\frac{1 - 18s^2 + 54(1 - e^2)s^4}{(1 - 12s^2)^{3/2}} = \frac{(2 - k^2)(1 + k^2)(1 - 2k^2)}{2(1 - k^2 + k^4)^{3/2}} \quad (38)$$

$$= \cos\theta. \quad (39)$$

The $\cos\theta$ of Eq. (39) is the same $\cos\theta$ that appears in Eq. (24), and, in particular, it is equal to 1, 0, -1 for $k^2 = 0, 1/2, 1$, respectively.

The curve represented by $k^2 = 1$, after setting $\cos\theta = -1$ in Eq. (39), can be readily shown to give a quadratic equation $27(1 - e^2)^2s^4 - 2(1 - 9e^2)s^2 - e^2 = 0$ that gives

$$s_1^2 = \frac{1 - 9e^2 + \sqrt{(1 - 9e^2)^2 + 27e^2(1 - e^2)^2}}{27(1 - e^2)^2} \quad (40)$$

for $e \neq 1$, and $s_1^2 = 1/16$ for $e = 1$. Equation (40) representing $k^2 = 1$ gives the upper boundary (for the values of s) of Region I (the uppermost heavy solid line in Fig. 1); it extends from $s_1 = \sqrt{2/27} = 0.272166$ for $e = 0$ to $s_1 = 1/4 = 0.250000$ for $e = 1$, i.e. a line that is nearly parallel to the e axis. Thus, Region I is a region bounded by $0 \leq s \leq s_1$ for $0 \leq e \leq \infty$ where s_1 is given by Eq. (40), in which the squared modulus of the elliptic functions that describe the orbits cover the entire range $0 \leq k^2 \leq 1$.

We now use Eq. (38) to give a plot of lines of constant $k^2 = 0.001, 0.01, 0.1, 0.3, \dots, 1$ as shown in Fig. 1. These lines conveniently divide Region I into regions of increasing field strengths as k^2 increases from 0 to 1. On a point representing a particular k^2 and a particular e value, s can be determined from Eq. (38) and the orbit is then given by Eq. (20) using Eqs. (A5), (10), and (21). The values of s on these constant k^2 lines for the values of $e = 0.1, 0.2, \dots, 1.0$ are given in Table I, which thus give the coordinates (e, s) of the points on the lines representing different values of k^2 . These coordinate points (e, s) from Table I are used to give the following tables: Tables II and III give the values of q_{\max} and q_{\min} for the orbits obtained from Eqs. (26) and (27). Note that the dimensionless distance q is in units of the Schwarzschild radius α which depends on the mass M of the star or black hole corresponding to that particular coordinate point, and thus one should not compare q at two different coordinate points just by their absolute values alone. Table IV presents the values of the precession angle in units of π , i.e. $\Delta\phi/\pi$, obtained from Eq. (25). Table V presents the values of the

TABLE I. Values of s for various values of e and k^2 in Region I.

s	$e = 0.0$	$e = 0.1$	$e = 0.2$	$e = 0.3$	$e = 0.4$	$e = 0.5$	$e = 0.6$	$e = 0.7$	$e = 0.8$	$e = 0.9$	$e = 1.0$
$k^2 = 0.001$	0.0554787	0.0454170	0.0346617	0.0286392	0.0248892	0.0222952	0.0203686	0.0188667	0.0176539	0.0166480	0.0157963
$k^2 = 0.01$	0.114809	0.109191	0.0969713	0.0851063	0.0757980	0.0686999	0.0631762	0.0587575	0.0551328	0.0520954	0.0495050
$k^2 = 0.1$	0.210213	0.208385	0.203281	0.195887	0.187374	0.178683	0.170376	0.162703	0.155729	0.149428	0.143740
$k^2 = 0.2$	0.238703	0.237612	0.234488	0.229734	0.223875	0.217424	0.210787	0.204236	0.197932	0.191956	0.186339
$k^2 = 0.3$	0.252575	0.251809	0.249595	0.246160	0.241814	0.236873	0.231612	0.226239	0.220900	0.215689	0.210663
$k^2 = 0.4$	0.260533	0.259944	0.258236	0.255562	0.252131	0.248163	0.243857	0.239372	0.234829	0.230311	0.225877
$k^2 = 0.5$	0.265408	0.264926	0.263523	0.261314	0.258458	0.255122	0.251460	0.247600	0.243642	0.239658	0.235702
$k^2 = 0.6$	0.268462	0.268045	0.266831	0.264913	0.262422	0.259494	0.256258	0.252821	0.249269	0.245666	0.242061
$k^2 = 0.7$	0.270350	0.269973	0.268875	0.267137	0.264873	0.262203	0.259239	0.256076	0.252791	0.249443	0.246076
$k^2 = 0.8$	0.271452	0.271099	0.270069	0.268436	0.266305	0.263787	0.260985	0.257986	0.254863	0.251671	0.248452
$k^2 = 0.9$	0.272006	0.271665	0.270668	0.269088	0.267025	0.264583	0.261863	0.258948	0.255908	0.252796	0.249653
$k^2 = 1.0$	0.272166	0.271828	0.270840	0.269276	0.267232	0.264812	0.262116	0.259225	0.256209	0.253120	0.250000

TABLE II. Values of q_{\max} for various values of e and k^2 in Region I.

q_{\max}	$e = 0.0$	$e = 0.1$	$e = 0.2$	$e = 0.3$	$e = 0.4$	$e = 0.5$	$e = 0.6$	$e = 0.7$	$e = 0.8$	$e = 0.9$	$e = 1.0$
$k^2 = 0.001$	174.74	273.42	522.17	871.99	1345.9	2012.0	3012.8	4681.4	8018.4	18025	∞
$k^2 = 0.01$	43.673	49.688	68.266	99.742	145.78	212.38	313.52	482.96	822.60	1842.4	∞
$k^2 = 0.1$	14.306	14.851	16.550	19.608	24.429	31.802	43.389	63.171	103.21	223.98	∞
$k^2 = 0.2$	11.377	11.697	12.693	14.481	17.300	21.627	28.458	40.168	63.938	135.75	∞
$k^2 = 0.3$	10.282	10.534	11.314	12.713	14.914	18.291	23.625	32.774	51.357	107.53	∞
$k^2 = 0.4$	9.7280	9.9479	10.630	11.849	13.766	16.704	21.342	29.298	45.460	94.318	∞
$k^2 = 0.5$	9.4118	9.6145	10.243	11.365	13.128	15.828	20.089	27.397	42.239	87.109	∞
$k^2 = 0.6$	9.2220	9.4148	10.012	11.078	12.751	15.314	19.356	26.285	40.359	82.903	∞
$k^2 = 0.7$	9.1078	9.2946	9.8733	10.906	12.527	15.008	18.920	25.627	39.246	80.413	∞
$k^2 = 0.8$	9.0421	9.2256	9.7938	10.808	12.399	14.833	18.672	25.252	38.612	78.997	∞
$k^2 = 0.9$	9.0094	9.1912	9.7542	10.759	12.335	14.747	18.549	25.066	38.299	78.296	∞
$k^2 = 1.0$	9.0000	9.1814	9.7429	10.745	12.317	14.722	18.514	25.013	38.209	78.095	∞

TABLE III. Values of q_{\min} for various values of e and k^2 in Region I.

q_{\min}	$e = 0.0$	$e = 0.1$	$e = 0.2$	$e = 0.3$	$e = 0.4$	$e = 0.5$	$e = 0.6$	$e = 0.7$	$e = 0.8$	$e = 0.9$	$e = 1.0$
$k^2 = 0.001$	149.15	215.27	343.84	466.77	574.79	669.11	751.92	825.10	890.20	948.48	1001.0
$k^2 = 0.01$	31.135	33.980	41.469	50.945	60.399	69.110	76.948	83.963	90.248	95.899	101.00
$k^2 = 0.1$	7.0549	7.1489	7.4154	7.8125	8.2864	8.7891	9.2876	9.7635	10.209	10.621	11.000
$k^2 = 0.2$	4.7480	4.7753	4.8530	4.9703	5.1133	5.2691	5.4278	5.5830	5.7311	5.8703	6.0000
$k^2 = 0.3$	3.8359	3.8465	3.8765	3.9220	3.9777	4.0389	4.1018	4.1639	4.2237	4.2803	4.3333
$k^2 = 0.4$	3.3289	3.3325	3.3428	3.3583	3.3773	3.3983	3.4199	3.4413	3.4619	3.4815	3.5000
$k^2 = 0.5$	3.0000	3.0000	3.0000	3.0000	3.0000	3.0000	3.0000	3.0000	3.0000	3.0000	3.0000
$k^2 = 0.6$	2.7667	2.7645	2.7585	2.7494	2.7382	2.7260	2.7134	2.7009	2.6889	2.6774	2.6667
$k^2 = 0.7$	2.5911	2.5877	2.5778	2.5629	2.5446	2.5247	2.5042	2.4840	2.4645	2.4460	2.4286
$k^2 = 0.8$	2.4535	2.4491	2.4366	2.4178	2.3949	2.3698	2.3442	2.3189	2.2946	2.2716	2.2500
$k^2 = 0.9$	2.3422	2.3371	2.3228	2.3012	2.2751	2.2465	2.2174	2.1887	2.1613	2.1354	2.1111
$k^2 = 1.0$	2.2500	2.2445	2.2288	2.2052	2.1767	2.1458	2.1142	2.0833	2.0538	2.0259	2.0000

TABLE IV. Values of $\Delta\phi/\pi$ for various values of e and k^2 in Region I.

$\Delta\phi/\pi$	$e = 0.0$	$e = 0.1$	$e = 0.2$	$e = 0.3$	$e = 0.4$	$e = 0.5$	$e = 0.6$	$e = 0.7$	$e = 0.8$	$e = 0.9$	$e = 1.0$
$k^2 = 0.001$	0.018906	0.012572	0.0072747	0.0049522	0.0037347	0.0029941	0.0024975	0.0021419	0.0018748	0.0016669	0.0015004
$k^2 = 0.01$	0.088019	0.078760	0.060819	0.046033	0.036087	0.029413	0.024739	0.021316	0.018713	0.016671	0.015029
$k^2 = 0.1$	0.42211	0.41041	0.37969	0.33964	0.29902	0.26259	0.23177	0.20625	0.18522	0.16780	0.15323
$k^2 = 0.2$	0.69762	0.68449	0.64888	0.59968	0.54604	0.49423	0.44737	0.40639	0.37108	0.34079	0.31478
$k^2 = 0.3$	0.95650	0.94206	0.90245	0.84652	0.78377	0.72123	0.66290	0.61042	0.56410	0.52353	0.48808
$k^2 = 0.4$	1.2200	1.2043	1.1608	1.0987	1.0281	0.95649	0.88857	0.82648	0.77085	0.72150	0.67786
$k^2 = 0.5$	1.5029	1.4858	1.4383	1.3701	1.2917	1.2116	1.1348	1.0638	0.99972	0.94234	0.89123
$k^2 = 0.6$	1.8226	1.8038	1.7519	1.6770	1.5905	1.5015	1.4157	1.3360	1.2635	1.1982	1.1398
$k^2 = 0.7$	2.2072	2.1866	2.1293	2.0465	1.9507	1.8517	1.7559	1.6666	1.5851	1.5114	1.4453
$k^2 = 0.8$	2.7169	2.6938	2.6295	2.5365	2.4286	2.3170	2.2087	2.1075	2.0150	1.9312	1.8558
$k^2 = 0.9$	3.5401	3.5129	3.4374	3.3281	3.2011	3.0696	2.9419	2.8224	2.7130	2.6139	2.5247
$k^2 = 1.0$	∞										

true eccentricity ε obtained from Eq. (28). Tables II, III, IV, and V are to be used in conjunction with Table I for identifying the locations (e, s) of the corresponding quantities that are presented. The physical quantities presented in Tables II, III, IV, and V together with the coordinates (e, s) given in Table I now give all possible periodic orbits in the Schwarzschild geometry in its entirety. That is, the

coordinates (e, s) of a planet orbiting a nonspinning black hole can be identified if the observation data on r_{\min} , r_{\max} , ε and $\Delta\phi$ can be collected. Region I shown in Fig. 1 is where orbits given by Eqs. (20) and (29) apply. In Secs. IV and V, we shall discuss Regions II and II', which are shown above Region I in Fig. 2 where orbits given by Eq. (36) apply. As an example of application of Tables I, II, III, IV,

TABLE V. Values of ϵ for various values of e and k^2 in Region I.

ϵ	$e = 0.0$	$e = 0.1$	$e = 0.2$	$e = 0.3$	$e = 0.4$	$e = 0.5$	$e = 0.6$	$e = 0.7$	$e = 0.8$	$e = 0.9$	$e = 1.0$
$k^2 = 0.001$	0.079005	0.11900	0.20592	0.30268	0.40148	0.50088	0.60054	0.70032	0.80015	0.90002	1
$k^2 = 0.01$	0.16760	0.18774	0.24420	0.32383	0.41413	0.50896	0.60587	0.70380	0.80227	0.90105	1
$k^2 = 0.1$	0.33947	0.35009	0.38115	0.43017	0.49343	0.56695	0.64738	0.73227	0.81998	0.90946	1
$k^2 = 0.2$	0.41109	0.42021	0.44683	0.48894	0.54373	0.60819	0.67964	0.75594	0.83548	0.91710	1
$k^2 = 0.3$	0.45659	0.46503	0.48963	0.52845	0.57889	0.63825	0.70412	0.77454	0.84802	0.92344	1
$k^2 = 0.4$	0.49009	0.49813	0.52152	0.55832	0.60598	0.66190	0.72378	0.78978	0.85847	0.92880	1
$k^2 = 0.5$	0.51659	0.52436	0.54692	0.58231	0.62797	0.68133	0.74014	0.80261	0.86737	0.93341	1
$k^2 = 0.6$	0.53845	0.54603	0.56798	0.60232	0.64644	0.69778	0.75410	0.81364	0.87508	0.93743	1
$k^2 = 0.7$	0.55703	0.56445	0.58594	0.61944	0.66233	0.71200	0.76623	0.82327	0.88183	0.94096	1
$k^2 = 0.8$	0.57314	0.58044	0.60155	0.63437	0.67623	0.72449	0.77692	0.83179	0.88781	0.94410	1
$k^2 = 0.9$	0.58733	0.59454	0.61534	0.64759	0.68857	0.73560	0.78645	0.83939	0.89316	0.94690	1
$k^2 = 1.0$	0.60000	0.60713	0.62766	0.65942	0.69963	0.74558	0.79502	0.84623	0.89798	0.94943	1

and V, from the second row and second column of Tables I, II, III, IV, and V and using only two significant figures, for orbits with $e = 0.10$, $s = 0.11$, $k^2 = 0.010$, we find from Tables II, III, IV, and V that $q_{\max} = 50$, $q_{\min} = 34$, $\Delta\phi/\pi = 0.079$ or $\Delta\phi = 14^\circ$, and $\epsilon = 0.19$, i.e. orbits with those seemingly small values of s and k^2 give a precession angle of 14° per revolution that is already very large compared to those encountered in our Solar System for which the precession angle is only $3.8''$ per century for the Earth's orbit (for which $s \approx 0.983 \times 10^{-4}$, $k^2 \approx 0.657 \times 10^{-9}$, $\epsilon \approx e \approx 0.017$), and the value of the true eccentricity ϵ of these orbits is already quite different from their energy parameter e . We thus appreciate that the range of values for s given by $0 \leq s \leq s_1$ for Region I, where s_1 ranges from 0.276 166 for $e = 0$ to 0.25 for $e = 1$, is not as small as it seems (noting also that $0 \leq k^2 \leq 1$), and that the classical Newtonian orbits are restricted to a very narrow strip of the region indeed for which $s \approx 0$ and $k^2 \approx 0$, and for which $\epsilon \approx e$ for $0 \leq e \leq 1$.

Although the lines of constant k^2 in Region I conveniently associate the orbits with the orbit equations for the periodic and terminating orbits given by Eqs. (20) and (29) and with the physical parameters given in Tables II, III, IV,

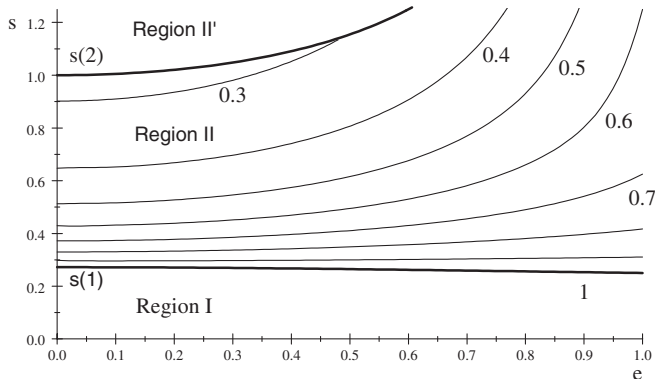


FIG. 2. Region II plots of $k^2 = 1.0, 0.9, 0.8, 0.7, 0.6, 0.5, 0.4, 0.3$.

and V, the precession angle $\Delta\phi$ and the true eccentricity ϵ are more physically meaningful parameters that can be associated with the description of the orbit. The expressions for $\Delta\phi$ and ϵ in terms of k and s are given by Eq. (A6) in Appendix A and Eq. (B1) in Appendix B. For a given value of $\Delta\phi$ and of e , we can use Eqs. (A6) and (38) to solve for s (and k) [using a numerical program such as FSOLVE in MAPLE] and thus locate its coordinate (e, s) ; and similarly for a given value of ϵ and of e , we can use Eqs. (B1) and (38) to solve for s (and k). The relationship of e and s with ϵ is simpler for $k^2 = 1$ and will be discussed later [see Eqs. (49) and (50)]. In Fig. 3, we present lines of constant $\Delta\phi/\pi$ (that are nearly horizontal) and lines of constant ϵ (that are bent vertical) in Region I, and the corresponding tables for their coordinates are

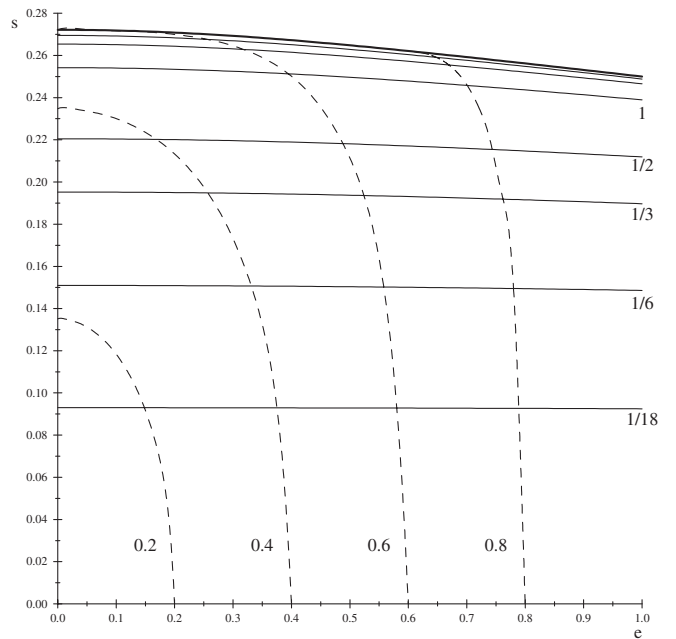


FIG. 3. $\Delta\phi/\pi = 1/18, 1/6, 1/3, 1/2, 1, 3/2, 2$ and $\epsilon = 0.2, 0.4, 0.6, 0.8$ (Region I).

presented in Tables VI and VII. We note that because $\Delta\phi$ given by Eq. (25) depends on γ given by Eq. (21) as well as on $K(k)$, the line of constant $\Delta\phi$ does not coincide with the line of constant k^2 except for $k^2 = 1$. We note also that the line of constant ε does not coincide with the (vertical) line of constant e except for $\varepsilon = e = 1$. We show in Appendix B that it is only for a very thin strip of region, where s is between zero and some very small positive value, that $\varepsilon \simeq e$ which applies in the Newtonian limit. We also show in Appendix B that $\varepsilon = e$ when $e = 1$ exactly. The distinction between e defined by Eq. (11) or Eq. (13) with ε defined by Eq. (28) in the Newtonian or non-Newtonian theory has never been clearly recognized previously.

With Fig. 3, which has curves of constant $\Delta\phi/\pi$ and constant ε in place, Region I is now partitioned into cells with the coordinate points specified by $(\Delta\phi/\pi, \varepsilon)$. We have a clear idea what the orbits of a planet would be like at points within each cell in terms of their precession angle and true eccentricity, and the coordinates of these orbits (e, s) then give the energy and field parameters corresponding to these orbits. In Fig. 4, we present examples of periodic and unbounded orbits, plotted in polar coordinates (q, ϕ) , corresponding to various precession angles of $\pi/6, \pi/3, \pi/2, \pi, 3\pi/2, 2\pi, \infty$ (vertically from top to bottom) for values of $e = 0, 0.5, 1$ (horizontally from left to right), where the star or black hole is located at the origin. We first

note that the orbits for which $e < 1$ are periodic and closed because f is a rational number in $\Delta\phi = f\pi$ for each one of them. The precession angle can be seen from the heavy solid line that marks the trajectory (as ϕ increases) from the initial point at $\phi = 0$ to the first point at which the distance from the origin is equal to the distance at $\phi = 0$. The true eccentricity of the orbits is ε given by Eq. (28). For example, for the orbit of Fig. 4 (a1) for $\Delta\phi = \pi/6, e = 0, \varepsilon$ is far from zero which can be seen from the q_{\min} and q_{\max} in the figure, and it can be more accurately calculated to be equal to 0.22 629. For each of the unbounded orbits characterized by $e = 1$, the incoming trajectory coming from infinity at $\phi = 0$ makes an angle ϕ with the outgoing trajectory going to infinity given by $\phi = 2K(k)/\gamma = 2\pi + \Delta\phi$ from Eq. (25), as can be seen in some of the figures presented. The case $\Delta\phi/\pi = \infty$ corresponding to the special case of $k^2 = 1$ will be discussed later in this section for which the planet starting from q_{\max} ends up circling the black hole with a radius that approaches q_{\min} (see Fig. 4(g)).

Generally, if we are given a coordinate point in Fig. 3, for example, a point on $e = 0.5$ just above the $\Delta\phi/\pi = 1/3$ line slightly to the left of the $\varepsilon = 0.6$ curve (where $\varepsilon = 0.581\,431\dots$ and $s = 0.194\,229\dots$), then we find $\Delta\phi = 60.4706\dots$ degrees or $\Delta\phi/\pi = 0.33\,594\dots$, and part of the orbit is shown in Fig. 5. Whether the orbit will close on itself depends on whether $\Delta\phi/\pi$ is or is not a rational

TABLE VI. Values of s for constant values of $\Delta\phi$ in Region I.

s	$e = 0.0$	$e = 0.1$	$e = 0.2$	$e = 0.3$	$e = 0.4$	$e = 0.5$	$e = 0.6$	$e = 0.7$	$e = 0.8$	$e = 0.9$	$e = 1.0$
$\Delta\phi = \pi/18$	0.0929 975	0.0929 922	0.0929 763	0.0929 498	0.0929 129	0.0928 655	0.0928 078	0.0927 400	0.0926 622	0.0925 745	0.0924 773
$\Delta\phi = \pi/6$	0.150 971	0.150 946	0.150 871	0.150 747	0.150 574	0.150 353	0.150 087	0.149 776	0.149 424	0.149 031	0.148 601
$\Delta\phi = \pi/3$	0.195 246	0.195 185	0.195 000	0.194 694	0.194 273	0.193 741	0.193 104	0.192 372	0.191 551	0.190 651	0.189 680
$\Delta\phi = \pi/2$	0.220 477	0.220 377	0.220 080	0.219 591	0.218 920	0.218 080	0.217 085	0.215 951	0.214 696	0.213 336	0.211 888
$\Delta\phi = \pi$	0.254 214	0.254 018	0.253 437	0.252 492	0.251 216	0.249 650	0.247 838	0.245 823	0.243 650	0.241 354	0.238 971
$\Delta\phi = 3\pi/2$	0.265 371	0.265 111	0.264 346	0.263 113	0.261 468	0.259 478	0.257 210	0.254 729	0.252 091	0.249 347	0.246 537
$\Delta\phi = 2\pi$	0.269 502	0.269 206	0.268 334	0.266 938	0.265 091	0.262 877	0.260 379	0.257 671	0.254 819	0.25 1875	0.248 804
$\Delta\phi = \infty$	0.272 166	0.271 828	0.270 840	0.269 276	0.267 232	0.264 812	0.262 116	0.259 225	0.256 209	0.253 120	0.250 000

TABLE VII. Values of s for constant values of ε in Region I

s	$e = 0.00$	$e = 0.02$	$e = 0.04$	$e = 0.06$	$e = 0.08$	$e = 0.10$	$e = 0.12$	$e = 0.14$	$e = 0.16$	$e = 0.18$	$e = 0.20$
$\varepsilon = 0.2$	0.135 153	0.13 4536	0.132 663	0.129 457	0.124 776	0.118 388	0.109 916	0.098 7083	0.0835 085	0.0611 485	0
s	$e = 0.00$	$e = 0.04$	$e = 0.08$	$e = 0.12$	$e = 0.16$	$e = 0.20$	$e = 0.24$	$e = 0.28$	$e = 0.32$	$e = 0.36$	$e = 0.40$
$\varepsilon = 0.4$	0.234 806	0.234 069	0.231 803	0.227 832	0.221 831	0.213 264	0.201 255	0.184 309	0.159 570	0.120 022	0
s	$e = 0.00$	$e = 0.06$	$e = 0.12$	$e = 0.18$	$e = 0.24$	$e = 0.30$	$e = 0.36$	$e = 0.42$	$e = 0.48$	$e = 0.54$	$e = 0.60$
$\varepsilon = 0.6$	0.272 166	0.272 037	0.271 572	0.270 524	0.268 439	0.264 552	0.257 565	0.245 130	0.222 468	0.177 299	0
s	$e = 0.61$	$e = 0.62$	$e = 0.64$	$e = 0.66$	$e = 0.68$	$e = 0.70$	$e = 0.72$	$e = 0.74$	$e = 0.76$	$e = 0.78$	$e = 0.80$
$\varepsilon = 0.8$	0.261 834	0.261 450	0.259 987	0.257 309	0.252 931	0.246 121	0.235 710	0.219 699	0.194 219	0.149 735	0

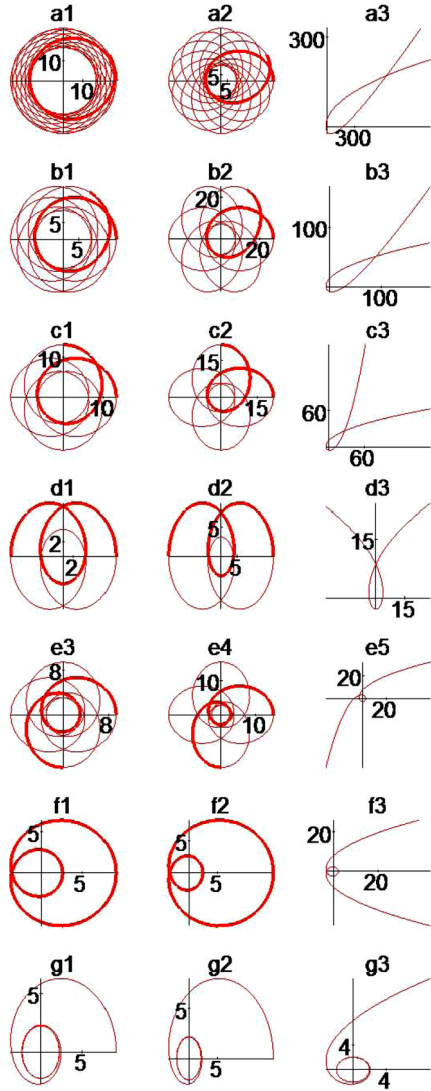


FIG. 4 (color online). Region I: Periodic (a1–f1, a2–f2), unbounded (a3–g3), asymptotic periodic orbits (g1–g3) for $\Delta\phi$ equal to (a) $\pi/6$, (b) $\pi/3$, (c) $\pi/2$, (d) π , (e) $3\pi/2$, (f) 2π , (g) ∞ and for e equal to (1) 0, (2) 0.5, (3) 1. The numbers on the axes are in units of Schwarzschild radii.

number in principle, even though, as we mentioned before, a truncated number in practice is always a rational number and the orbit will be a closed one. We only show part of the orbit in Fig. 5 as the subsequent path is clear from the angle of precession and true eccentricity of the orbit and we are not concerned with how many “leaves” the orbit is going to create. Figure 3 (or one with even more curves of constant $\Delta\phi/\pi$ and constant ϵ) is a very useful map that can be used fruitfully with any observation data that are obtained for any planet.

Besides the special case $k^2 = 1$, the case of $k^2 = 1/2$ is also somewhat special in that it allows many relationships to be expressed simply and explicitly. We present some of these simple relations for $k^2 = 1/2$ in Appendix C. It is to be noted from Fig. 1 that the line of constant $k^2 = 1/2$ is

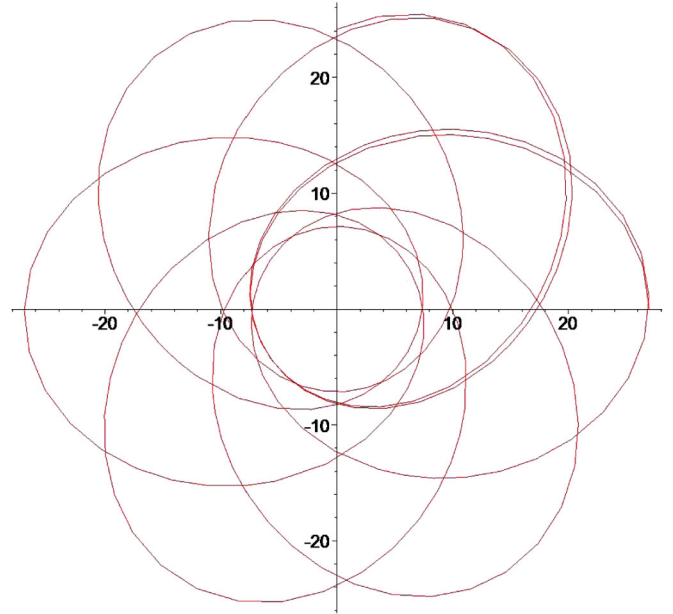


FIG. 5 (color online). Precessional orbit for $\Delta\phi = (\frac{1}{3} + 0.002614\dots)\pi$, $\epsilon = 0.58143\dots$, $e = 0.5$, $s = 0.194229\dots$. The numbers on the axes are in units of Schwarzschild radii.

very close to the boundary given by $k^2 = 1$. The line of constant $k^2 = 1/2$ for Region II, on the other hand, is closer to dividing the region approximately into two halves, as shown in Fig. 2. The $k^2 = 1/2$ curve for Region II will be discussed in Sec. IV.

The terminating orbits in Region I given by Eq. (29) can be characterized by the planet’s initial position q_1 given by Eq. (31), and by the angle ϕ_1 at which the planet enters the center of the black hole. It is interesting to note that even for these terminating orbits, the precession angle still has an “extended” meaning and use that we shall describe. It is clear from Eq. (29) that the orbit terminates, i.e. q becomes zero when $\gamma\phi_1 = K(k)$, but if the orbit is continued (by continuing to increase ϕ), q would assume its initial value at $\phi = 0$ when $\gamma\phi' = 2K(k)$, producing a “precession angle” of $\Delta\phi = \phi' - 2\pi = 2K(k)/\gamma - 2\pi$ which is equal to the precession angle for the corresponding periodic orbit at the same coordinate point (e, s) . Since $\phi' = 2\phi_1$, the polar angle ϕ_1 at which the path of the terminating orbit enters the center of the black hole is related simply to the precession angle of the periodic orbit by $\phi_1 = \Delta\phi/2 + \pi$, or

$$\frac{\phi_1}{\pi} = \frac{1}{2} \frac{\Delta\phi}{\pi} + 1.$$

As ϕ_1/π can be easily calculated from $\Delta\phi/\pi$ for the periodic orbits given in Table IV, we do not tabulate it separately. The values of q_1 are presented in Table VIII, and we note the small range $1 \leq q_1 \leq 2.25$ for the entire Region I. Examples of these terminating orbits are pre-

TABLE VIII. Values of q_1 for various values of e and k^2 in Region I (terminating orbits).

q_1	$e = 0.0$	$e = 0.1$	$e = 0.2$	$e = 0.3$	$e = 0.4$	$e = 0.5$	$e = 0.6$	$e = 0.7$	$e = 0.8$	$e = 0.9$	$e = 1.0$
$k^2 = 0.001$	1.0126	1.0084	1.0048	1.0033	1.0025	1.0020	1.0017	1.0014	1.0012	1.0011	1.0010
$k^2 = 0.01$	1.0582	1.0521	1.0403	1.0306	1.0240	1.0196	1.0165	1.0142	1.0124	1.0111	1.0100
$k^2 = 0.1$	1.2685	1.2614	1.2427	1.2180	1.1928	1.1699	1.1504	1.1341	1.1206	1.1094	1.1000
$k^2 = 0.2$	1.4255	1.4182	1.3983	1.3703	1.3394	1.3089	1.2810	1.2563	1.2348	1.2161	1.2000
$k^2 = 0.3$	1.5575	1.5502	1.5299	1.5007	1.4672	1.4332	1.4008	1.3711	1.3445	1.3209	1.3000
$k^2 = 0.4$	1.6756	1.6683	1.6481	1.6186	1.5841	1.5483	1.5135	1.4809	1.4511	1.4242	1.4000
$k^2 = 0.5$	1.7844	1.7773	1.7574	1.7281	1.6935	1.6570	1.6210	1.5869	1.5552	1.5263	1.5000
$k^2 = 0.6$	1.8864	1.8795	1.8601	1.8315	1.7973	1.7610	1.7248	1.6900	1.6575	1.6275	1.6000
$k^2 = 0.7$	1.9831	1.9764	1.9578	1.9301	1.8968	1.8612	1.8254	1.7908	1.7582	1.7279	1.7000
$k^2 = 0.8$	2.0754	2.0691	2.0513	2.0248	1.9929	1.9584	1.9236	1.8898	1.8577	1.8278	1.8000
$k^2 = 0.9$	2.1642	2.1583	2.1415	2.1164	2.0860	2.0532	2.0198	1.9872	1.9562	1.9271	1.9000
$k^2 = 1.0$	2.2500	2.2445	2.2288	2.2052	2.1767	2.1458	2.1142	2.0833	2.0538	2.0259	2.0000

sented in Fig. 6. The dotted line represents the continuation of the orbit when ϕ is continued beyond ϕ_1 .

Before we discuss Regions II and II', we want to describe three special cases: the case of $k^2 = 0$ which, as we shall see, is not of any interest but must be included for completeness; the case of $k^2 = 1$ which gives the upper boundary of Region I (and lower boundary of Region II); and the case of $e = 1$ (see Figs. 1 and 2).

(i) The Special Case of $k^2 = 0$

The line of $k^2 = 0$ coincides with the $s = 0$ axis in Fig. 1. To show this, we note that $k^2 = 0$ implies $\theta = 0$ from Eq. (A2). Substituting $\theta = 0$ into Eq. (24) gives $s = 0$ when we use the expressions in Eq. (10) for g_2 and g_3 . Then we find $g_2 = 1/12$ and $g_3 = 1/216$, and from Eq. (A5), we find

$$e_1 = \frac{1}{6}, \quad e_2 = e_3 = -\frac{1}{12},$$

and $\gamma = 1/2$. Equation (20) then gives $1/q = 0$ or $q = \infty$, i.e. it is the limiting case of zero gravitational field. As we pointed out earlier, the classical Newtonian case is given by only a very narrow strip represented by $k^2 \approx 0$ and $s \approx 0$ for which q is large but finite.

(ii) The Special Case of $k^2 = 1$

It follows from Eqs. (38) and (39) that on the line of $k^2 = 1$, $\cos\theta = -1$. Thus, from Eqs. (24) and (17), we have

$$\Delta = 0, \quad (41)$$

which can be identified as the ‘‘boundary’’ between Solutions (A) and (B) in Sec. II. The range of s values for $\Delta = 0$ is $0.25 \leq s \leq 0.272166$ for $1 \geq e \geq 0$ [see the discussion below Eq. (40)], and for that range of s values, $s < 1/2\sqrt{3} = 0.288675$ or $s^2 < 1/12$ and therefore $g_2 > 0$ [see Eq. (10)]. From Eq. (41), the relation between g_2 and g_3 can be more precisely expressed as

$$\sqrt[3]{g_3} = -\sqrt{\frac{g_2}{3}}$$

after noting that g_3 is negative and g_2 is positive for the

values of s along the line $k^2 = 1$. Also from Eq. (A5), we note that

$$e_1 = e_2 = \sqrt{\frac{g_2}{12}}, \quad e_3 = -\sqrt{\frac{g_2}{3}}. \quad (42)$$

Equation (20) becomes

$$\frac{1}{q} = \frac{1}{3} + 2\sqrt{\frac{g_2}{3}} \frac{1 - 5 \operatorname{sech}(2\gamma\phi)}{1 + \operatorname{sech}(2\gamma\phi)}, \quad (43)$$

where

$$\gamma = \left(\frac{3g_2}{4}\right)^{1/4} \quad (44)$$

and where the values of g_2 (and g_3) are those given by the values of e and s on the line $k^2 = 1$ that are obtained from Eq. (40). The orbit will be referred to as an asymptotic one. The planet starts from an initial position q_{\max} at $\phi = 0$ given by

$$\frac{1}{q_{\max}} = \frac{1}{3} + 4e_3 = \frac{1}{3} - 4\sqrt{\frac{g_2}{3}} \quad (45)$$

and ends up at $\phi = \infty$ circling the star or black hole with a radius that asymptotically approaches q_{\min} given by

$$\frac{1}{q_{\min}} = \frac{1}{3} + 4e_2 = \frac{1}{3} + 2\sqrt{\frac{g_2}{3}}. \quad (46)$$

Equations (43)–(46) are explicit and simple equations that give the orbit equation, q_{\max} , and q_{\min} for $k^2 = 1$. In particular, it is seen from Table III, for example, that q_{\min} ranges from 2 for $e = 0$ to $9/4 = 2.25$ for $e = 1$, i.e. q_{\min} is still no less than twice the Schwarzschild radius for the strongest gravitational field that permits the periodic orbits. However, it is a very small number indeed compared to, say, $q_{\min} \approx 5 \times 10^7$ for the Earth's orbit around the Sun.

On this upper boundary $k^2 = 1$ of Region I, the terminating orbit given by Eq. (29) from Solution (A2) becomes a circular orbit with a radius $q_c = q_1$, where q_1 is the initial distance of the planet from the star or black hole given by

Eq. (30). From Eqs. (30) and (31) and noting that $e_1 = e_2$ for $k^2 = 1$, we find that

$$q_c = q_1 = q_{\min} \quad (47)$$

given by Eq. (46) [see Tables III and VIII for $k^2 = 1$]. We shall refer to the orbits given by Eq. (43) as the asymptotic elliptic-type (for $0 \leq e < 1$), asymptotic parabolic-type (for $e = 1$) and asymptotic hyperbolic-type (for $e > 1$) orbits, and to the orbits given by Eq. (47) as the asymptotic terminating orbits, respectively, of Region I. Thus, the special cases given by Eqs. (43) and (47) for $k^2 = 1$ of the orbits given by Eqs. (20) and (29) for Solutions A1 and A2, respectively, clearly exhibit completely different behaviors from their counterparts for $0 \leq k^2 < 1$. Examples of asymptotic elliptic-type orbits are shown in Fig. 4 g1 and g2, and an example of asymptotic parabolic-type orbit is shown in Fig. 4 g3. Asymptotic terminating orbits are simply circles of radius equal to q_1 , as shown in Fig. 6(d).

Using Eqs. (28), (42), (45), and (46), for $k^2 = 1$ the true eccentricity ε can be shown to be expressible in terms of g_2 by

$$\varepsilon = \frac{9\sqrt{g_2/3}}{1 - 3\sqrt{g_2/3}}, \quad (48)$$

which can be solved to give s in terms of ε , and then e in terms of ε using Eq. (38). We find that the coordinates (e, s) of a given $0.6 \leq \varepsilon \leq 1$ on the line $k^2 = 1$ are given by

$$e = \frac{\sqrt{(1 + \varepsilon)(-3 + 5\varepsilon)}}{(3 - \varepsilon)}, \quad (49)$$

and

$$s = \frac{\sqrt{(3 - \varepsilon)(1 + \varepsilon)}}{2(3 + \varepsilon)}. \quad (50)$$

It is interesting that Eqs. (49) and (50) can be used in place of Eq. (40) as parametric equations for determining the coordinates (e, s) of the line $k^2 = 1$ as ε takes the values from 0.6 to 1. In particular, Eqs. (49) and (50) allow us to see that the $\varepsilon = \text{const}$ curves are not vertical (except for $\varepsilon = e = 1$), and they intersect the upper boundary s_1 of Region I for $0.6 \leq \varepsilon \leq 1$ (see Fig. 3). The $\varepsilon = 0.6$ curve, the boundary curve s_1 , and the s axis are concurrent at $e = 0$, $s = \sqrt{2/27}$. By looking at where the $\varepsilon = \text{const}$ curve intersects the $k^2 = 1$ curve for $0.6 \leq \varepsilon \leq 1$ using Eq. (49) and Fig. 3, for example, we can make conclusions such as periodic orbits with $e = 0$ have true eccentricity in the range $0 \leq \varepsilon \leq 0.6$, and periodic orbits with $e < 3\sqrt{5}/11 = 0.609836$ have $\varepsilon < 0.8$.

(iii) The Special Case of $e = 1$

The orbits corresponding to $e = 1$ given by Eq. (20) will be referred to as the parabolic-type orbits. In Appendix B, we show that $e = 1$ always gives an unbounded orbit except for the asymptotic terminating orbit of Region I,

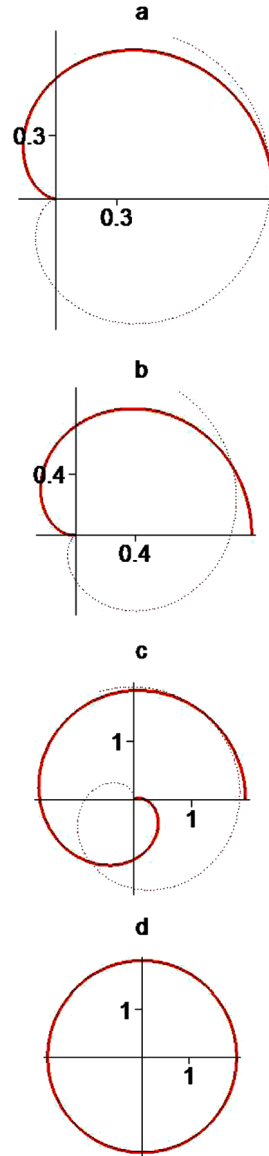


FIG. 6 (color online). Terminating orbits in Region I (dotted line represents trajectory beyond $r = 0$). (a) $k^2 = 0.01$, $e = 0$, $s = 0.114809$, $\frac{\varphi_1}{\pi} = 1.0440$, $q_1 = 1.0582$. (b) $k^2 = 0.1$, $e = 0.5$, $s = 0.178683$, $\frac{\varphi_1}{\pi} = 1.1313$, $q_1 = 1.1699$. (c) $k^2 = 0.9$, $e = 0.9$, $s = 0.252796$, $\frac{\varphi_1}{\pi} = 2.3070$, $q_1 = 1.9271$. (d) $k^2 = 1$, $e = 1$, $s = 0.25$, $\varphi_1 = \infty$, $q_1 = 2$.

which becomes a circular orbit with a radius given by Eq. (47) independent of e and thus is not an unbounded orbit. Many explicitly simple relationships among s , k , q_{\min} , q_1 , etc. have been found on the boundary line $e = 1$, and they are given and proved in Appendix B. In particular, we have, on $e = 1$ in Region I, that

$$s^2 = \frac{k^2}{4(1 + k^2)^2}, \quad (51)$$

$$\gamma = \left(\frac{1}{4(1 + k^2)} \right)^{1/2}, \quad (52)$$

$$q_{\min} = \frac{1 + k^2}{k^2}, \quad (53)$$

and

$$q_1 = 1 + k^2. \quad (54)$$

Examples of the orbits for $e = 1$ are shown in Fig. 4 (a3–g3).

We shall now describe Regions II and II' for the orbit Eq. (36) given by Solution B for the case $\Delta > 0$.

IV. REGIONS II AND II' FOR $0 \leq e \leq 1$

Consider the orbits expressed by Eq. (36) given by Solution B and characterized mathematically by $\Delta > 0$. The associated values for (e, s) in this case satisfy $s > s_1$, where s_1 is the upper boundary of Region I given by Eq. (40). We shall be mainly concerned with the values of e in the range $0 \leq e \leq 1$ in this section, and we shall deal with the case of $e > 1$ in the next section. This region of parameter space defined by $s > s_1$ can be naturally divided into two sectors which we call Region II and II' with Region II bordering Region I (see Fig. 2). The boundary between Regions II and II' is determined by the Schwarzschild radius in a manner to be described later in this section.

We first want to prove that the lower boundary (for s) of Region II, characterized by $\Delta = 0$ as it is for the upper boundary of Region I, also gives $k^2 = 1$, where k^2 is calculated from Eq. (35) for Solution (B) [In Sec. III, we showed that for k^2 calculated from Eq. (22) for Solution (A), $k^2 = 1$ implies $\Delta = 0$]. Substituting $\Delta = 0$ into Eq. (32) gives

$$A = B = \frac{1}{2} \sqrt[3]{g_3} = -\frac{1}{2} \sqrt{\frac{g_2}{3}}.$$

After noting that $A(=B)$ is a negative value for the range of s values for $\Delta = 0$, substituting the above into Eq. (35) gives $k^2 = 1$. We also find from Eq. (34) that $\gamma^2 = -3\sqrt[3]{g_3}/2 = \sqrt{3}g_2/2$ which agrees with the γ given by Eq. (44), and we find from Eq. (33) that

$$a = \sqrt[3]{g_3} = -\sqrt{\frac{g_2}{3}}. \quad (55)$$

Substituting these into Eq. (36) gives the same orbit Eq. (43) for the terminating orbit in Region II on its lower boundary as that for the asymptotic periodic orbit in Region I on its upper boundary. Thus, on the boundary $k^2 = 1$ the equation for the orbits in Region II does not represent a terminating orbit but is the same as the asymptotic periodic orbit for Region I given by Eq. (43) [see Fig. 4, g1–g3]. Also, from Eqs. (42) and (55), we see that the smallest root in Eq. (23) in Solution (A) is identified with the real root given by Eq. (33) of Solution (B), i.e. $e_3 = a$. Thus, from Eqs. (26) and (37), $q_2 = q_{\max}$ when $k^2 = 1$, i.e. the initial distance q_2 of the terminating orbit in

Region II can be identified as the continuation of q_{\max} of the periodic orbit from Region I. On the boundary of Regions I and II, the two other real roots $e_1 = e_2$ given by Eq. (42) of the cubic Eq. (16) agree with $b = \bar{b}$ given below Eq. (33). The line $k^2 = 1$ defined by Eq. (40) is the boundary between Regions I and II; it is the upper boundary for Region I and is the lower boundary for Region II (see Fig. 2). The above discussion also illustrates the transition that takes place: from a periodic orbit to an asymptotic periodic orbit to a terminating orbit, as one crosses the boundary from Region I to II.

We now consider the upper boundary of Region II. We define this boundary to be that obtained by requiring the planet's initial position to be just at the Schwarzschild horizon, i.e. that obtained by setting $q = 1$ initially at $\phi = 0$. Setting $q = 1$ in Eq. (36) for $\phi = 0$, which is $1/q = 1/3 + 4a$, we require $a = 1/6$, where a is the real root of the cubic Eq. (16). We then use the equation

$$4\left(\frac{1}{6}\right)^3 - \left(\frac{1}{6}\right)g_2 - g_3 = 0, \quad (56)$$

and substitute the expressions for g_2 and g_3 given in Eq. (10) into Eq. (56) and solve for s . We find

$$s_2^2 = \frac{1}{1 - e^2}, \quad (57)$$

which we shall use as the equation for the upper boundary of Region II, for $0 \leq e \leq 1$. Thus, Region II is a region bounded between $e = 0$ and $e = 1$, and between s_1 given by Eq. (40) [the lower heavy solid line in Fig. 2] and s_2 given by Eq. (57) [the upper heavy solid line in Fig. 2], i.e. $s_1 < s \leq s_2$. The region defined by $s_2 < s \leq \infty$ and bounded between $e = 0$ and $e = 1$ will be called Region II', for which the planet's initial position ranges from just inside the Schwarzschild horizon up to the center of the black hole. Since the same terminating orbit Eq. (36) applies in Regions II and II', the division into two regions may seem unnecessary. However, the Schwarzschild radius is of physical significance, and it is useful to know the location of the curve s_2 in the (e, s) plot, which indicates that the initial position of the planet is at the Schwarzschild horizon. Separating out Region II' also makes it possible to realize and appreciate that a very large region of the characterizing parameter $s_2 < s \leq \infty$ is of relevance only to a very small physical region $0 \leq q < 1$ for the case where the initial position of the planet is inside the Schwarzschild horizon.

For Region II, as s increases its value above those on its lower boundary $s = s_1$ on which $k^2 = 1$, the value of k^2 calculated from Eq. (35) decreases from 1. The curves of constant k^2 for $k^2 = 0.9, 0.8, \dots$ can be easily obtained from Eq. (35) where A and B are expressed in terms of s and e (again using MAPLE FSOLVE), and they are presented in Fig. 2. However, the value of k^2 has a minimum value that is not 0 in Region II. First, we show in Appendix C that the $k^2 = 1/2$ curve is given by

$$s^2 = \frac{1}{6(1 - e^2)} \left(1 + \sqrt{\frac{1 + 2e^2}{3}} \right). \quad (58)$$

$$\frac{\phi_2}{\pi} = \frac{1}{2} \frac{\Delta\phi}{\pi} + 1. \quad (59)$$

The significance of this $k^2 = 1/2$ curve is that on it, as $e \rightarrow 1, s \rightarrow \infty$, just like the curve for the upper boundary of Region II represented by Eq. (57). For $k^2 > 0.5$, the constant k^2 curves intersect the $e = 1$ line at some finite value of s , whereas for $k^2 < 0.5$, the constant k^2 curves intersect the upper boundary curve given by Eq. (57) at points for which the values of e are less than 1. We then find that the minimum value of k^2 in Region II is equal to $1/2 - 1/(2\sqrt{5}) = 0.276393$, which is obtained by setting $e = 0, s = 1$ in Eqs. (32) and (35), and this value of k^2 appears at one coordinate point only at $e = 0$ and $s = 1$. There is no orbit whose k^2 is less than 0.276393 in Region II (see Fig. 2), and k^2 is thus restricted to the range $0.276393 \leq k^2 \leq 1$.

In Table IX, we present the coordinates (e, s) of these curves of constant k^2 between 0.276393 and 1. In Table X, we present the values of q_2 given by Eq. (37), the initial distance of the planet from the black hole. Note that unlike q_1 for the terminating orbits in Region I whose range is finite and small, q_2 can be infinite (for $e = 1$ and $k^2 > 0.5$). Like the terminating orbits of Region I, the terminating orbits of Region II can be characterized by q_2 and the angle ϕ_2 at which the planet enters the center of the black hole. If we define the ‘‘precession angle’’ $\Delta\phi$ for the terminating orbits as in Eq. (25), with k and γ defined by Eqs. (35) and (34), then $\phi_2 = K(k)/\gamma = \Delta\phi/2 + \pi$, or

In Table XI, we present the values of ϕ_2 . Tables X and XI are to be used in conjunction with Table IX that give the coordinates of the constant k^2 curves. Examples of these terminating orbits obtained from Eq. (36) are shown in Figs. 7(b)–7(d). Again the dotted line shows the continuation of the orbit beyond ϕ_2 . A planet coming from very far away, i.e. an unbounded orbit with $e = 1$, with an initial trajectory perpendicular to the line joining it to the black hole, can terminate at the black hole; the condition for this to happen is $s > 0.25$. Figures 8(a)–8(c) show three unbounded orbits ($e = 1$) as s increases from just below to just above the critical field parameter $s = 0.25$. Figure 8(a) also shows an example of a precession angle in which the planet makes more than three revolutions around a black hole before assuming a distance equal to its initial distance (which is infinity) from the black hole. As noted after Eq. (25), the actual precession angle in this case should be more appropriately given by $2K(k)/\gamma - 6\pi$ which can be obtained from the presented value of $\Delta\phi/\pi = 4.6378$ [where $\Delta\phi$ is defined by Eq. (25)] and gives 0.6378π . Thus, for Fig. 8(a), 0.6378π gives the angle between the initial incoming trajectory from very far away at $\phi = 0$ and the final outgoing trajectory going to infinity, i.e. 0.6378π is the polar angle of the direction of the outgoing trajectory going to infinity with respect to the x axis (but we have not extended the outgoing trajectory far enough to show the accuracy of this angle).

TABLE IX. Values of s for various values of e and k^2 in Region II.

s	$e = 0.0$	$e = 0.1$	$e = 0.2$	$e = 0.3$	$e = 0.4$	$e = 0.5$	$e = 0.6$	$e = 0.7$	$e = 0.8$	$e = 0.9$	$e = 1.0$
$k^2 = 1.0$	0.272 166	0.271 828	0.270 840	0.269 276	0.267 232	0.264 812	0.262 116	0.259 225	0.256 209	0.253 120	0.250 000
$k^2 = 0.9$	0.297 739	0.297 917	0.298 442	0.299 293	0.300 443	0.301 865	0.303 537	0.305 444	0.307 575	0.309 927	0.312 500
$k^2 = 0.8$	0.329 945	0.330 718	0.333 024	0.336 843	0.342 169	0.349 050	0.357 613	0.368 098	0.380 913	0.396 727	0.416 667
$k^2 = 0.7$	0.371 926	0.373 406	0.377 868	0.385 401	0.396 232	0.410 826	0.430 060	0.455 531	0.490 285	0.540 844	0.625 000
$k^2 = 0.6$	0.429 234	0.431 592	0.438 767	0.451 100	0.469 328	0.494 871	0.530 424	0.581 374	0.659 978	0.802 847	1.25 000
$k^2 = 0.5$	0.512 730	0.516 250	0.527 046	0.545 908	0.574 478	0.615 920	0.676 462	0.769 603	0.930 895	1.30 267	-
$k^2 = 0.4$	0.646 974	0.652 192	0.668 307	0.696 858	0.741 019	0.806 949	0.907 116	1.07 001	1.37 756	2.21 530	-
$k^2 = 0.3$	0.901 890	0.910 054	0.935 412	0.980 848	1.05 231	-	-	-	-	-	-

TABLE X. Values of q_2 for various values of e and k^2 in Region II.

q_2	$e = 0.0$	$e = 0.1$	$e = 0.2$	$e = 0.3$	$e = 0.4$	$e = 0.5$	$e = 0.6$	$e = 0.7$	$e = 0.8$	$e = 0.9$	$e = 1.0$
$k^2 = 1.0$	9.0000	9.1814	9.7429	10.745	12.317	14.722	18.514	25.013	38.209	78.095	∞
$k^2 = 0.9$	7.6760	7.7965	8.1685	8.8291	9.8596	11.426	13.833	18.073	26.550	52.109	∞
$k^2 = 0.8$	6.4074	6.4806	6.7060	7.1041	7.7200	8.6471	10.084	12.507	17.353	31.823	∞
$k^2 = 0.7$	5.1997	5.2381	5.3557	5.5620	5.8780	6.3467	7.0597	8.2346	10.522	17.148	∞
$k^2 = 0.6$	4.0606	4.0750	4.1191	4.1959	4.3120	4.4809	4.7310	5.1276	5.8592	7.8120	∞
$k^2 = 0.5$	3.0000	3.0000	3.0000	3.0000	3.0000	3.0000	3.0000	3.0000	3.0000	3.0000	-
$k^2 = 0.4$	2.0324	2.0259	2.0059	1.9717	1.9217	1.8523	1.7574	1.6241	1.4235	1.0692	-
$k^2 = 0.3$	1.1805	1.1733	1.1516	1.1148	1.0618	-	-	-	-	-	-

TABLE XI. Values of ϕ_2/π for various values of e and k^2 in Region II.

ϕ_2/π	$e = 0.0$	$e = 0.1$	$e = 0.2$	$e = 0.3$	$e = 0.4$	$e = 0.5$	$e = 0.6$	$e = 0.7$	$e = 0.8$	$e = 0.9$	$e = 1.0$
$k^2 = 1.0$	∞										
$k^2 = 0.9$	2.6599	2.6469	2.6099	2.5551	2.4890	2.4176	2.3448	2.2733	2.2043	2.1385	2.0761
$k^2 = 0.8$	2.1586	2.1480	2.1175	2.0711	2.0132	1.9479	1.8781	1.8055	1.7309	1.6541	1.5742
$k^2 = 0.7$	1.8169	1.8079	1.7819	1.7412	1.6889	1.6274	1.5584	1.4822	1.3977	1.3010	1.1817
$k^2 = 0.6$	1.5360	1.5283	1.5060	1.4703	1.4231	1.3654	1.2977	1.2186	1.1237	1.0002	0.78496
$k^2 = 0.5$	1.2822	1.2758	1.2569	1.2262	1.1843	1.1315	1.0671	0.98815	0.88720	0.74053	-
$k^2 = 0.4$	1.0373	1.0321	1.0166	0.99105	0.95540	0.90923	0.85112	0.77757	0.68006	0.53257	-
$k^2 = 0.3$	0.78606	0.78213	0.77030	0.75047	0.72230	-	-	-	-	-	-

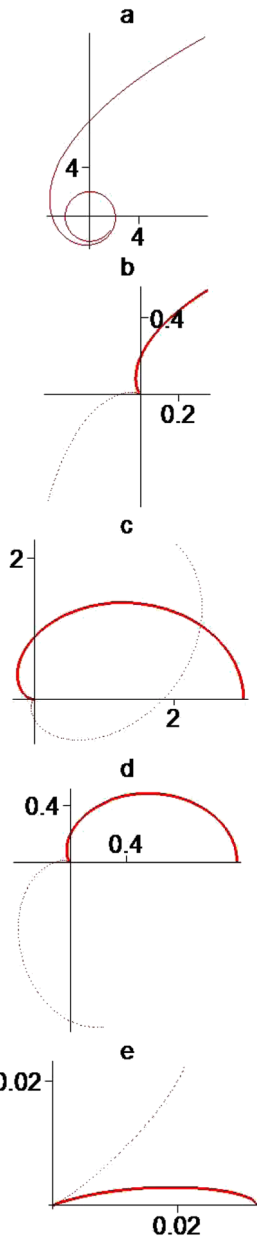


FIG. 7 (color online). Terminating orbits in Region II (a-d) and Region II' (e). (a) $k^2 = 1, e = 1, s = 0.25, \frac{\phi_2}{\pi} = \infty, q_2 = \infty$. (b) $k^2 = 0.6, e = 1, s = 1.25, \frac{\phi_2}{\pi} = 0.78496, q_2 = \infty$. (c) $k^2 = 0.5, e = 0.5, s = 0.615920, \frac{\phi_2}{\pi} = 1.1315, q_2 = 3$. (d) $k^2 = 0.3, e = 0, s = 0.901890, \frac{\phi_2}{\pi} = 0.78606, q_2 = 1.1805$. (e) $k^2 = 0.095385, e = 0, s = 10, \frac{\phi_2}{\pi} = 0.13684, q_2 = 0.03267$.

We now present some useful simple expressions for the following special cases.

(i) Special Case on the Upper Boundary of Region II Given By Eq. (57)

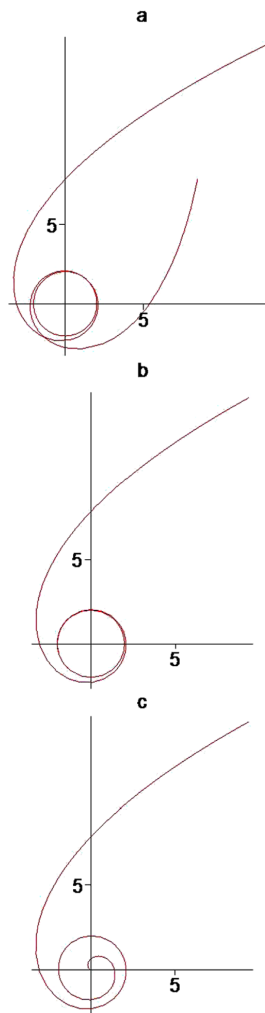


FIG. 8 (color online). Unbounded orbits for (a) $k^2 = 0.99, e = 1, s = 0.2499968435, \frac{\Delta\phi}{\pi} = 4.6378$. (b) $k^2 = 1, e = 1, s = 0.25, \frac{\Delta\phi}{\pi} = \infty$. (c) $k^2 = 0.9998000799, e = 1, s = 0.2501, \frac{\phi_2}{\pi} = 5.0816$.

We show in Appendix D that on the upper boundary of Region II given by Eq. (57), the values of k^2 and γ given by Eqs. (35) and (34) become

$$k^2 = \frac{1}{2} - \frac{1}{4\sqrt{1/3 - g_2}}, \quad (60)$$

$$\gamma = \left[\frac{1}{4} \left(\frac{1}{3} - g_2 \right) \right]^{1/4}, \quad (61)$$

where the s values for g_2 are given by Eq. (57).

(ii) Special Case for $e = 1$ of Region II

Just as for Region I, there are simple and interesting relations among k^2 , s and γ on the right boundary $e = 1$ of Region II, and they are shown in Appendix D. In particular, we have, on $e = 1$ in Region II, that for $s > 1/4$,

$$k^2 = \frac{1}{2} + \frac{1}{8s}, \quad (62)$$

or that, for $1 \geq k^2 > 1/2$,

$$s = \frac{1}{8(k^2 - 1/2)}, \quad (63)$$

and that

$$\gamma = \sqrt{\frac{s}{2}}. \quad (64)$$

Appendix E presents a special case given by $s^2 = 1/12$ in Region II that is notable, which has been associated with the case of so-called innermost stable circular orbit in the literature.

While we may call the entire sector $s > s_1$ given by Eq. (40) above Region I in Fig. 2 just one region that allows only terminating orbits given by Eq. (36), it is useful to divide it into Regions II and II' using the curve $s = s_2$ given by Eq. (57). Region II' is the region of parameter space in (e, s) for which $s > s_2$ and $0 \leq e < 1$. The heavy solid curve labeled s_2 in Fig. 2 delineates the boundary of Region II', which separates it from Region II. Despite the apparent large size of Region II', the terminating orbits here have little variety in the sense that the range of initial distances $q_{2'}$ that are given by $1/q_{2'} = 1/3 + 4a$ [see Eq. (37)], is limited ($0 \leq q_{2'} < 1$), and the range of the angle $\phi_{2'} = K(k)/\gamma$ at which the planet enters the black hole is also limited. It can be shown that the range of $\phi_{2'}$ is $0 \leq \phi_{2'} < 0.789\pi$. An example of a terminating orbit obtained from Eq. (36) in Region II' is shown as the solid line in Fig. 7(e); the dotted line shows the continuation of the orbit beyond $\phi_{2'}$. It may be of some mathematical interest to note that as $s \rightarrow \infty$ in Region II', the modulus of the Jacobian elliptic functions used to describe the orbits does not go to zero; instead $k^2 \rightarrow (2 - \sqrt{3})/4 = 0.0669873$, and thus k^2 in Region II' is restricted to the range $0.0669873 \leq k^2 < 0.5$.

The analytic orbit Eqs. (20) and (29) for $\Delta \leq 0$, and Eq. (36) for $\Delta > 0$, that we have considered for the case of

$0 \leq e \leq 1$, will now be considered for the case of $e > 1$ in the following section.

V. REGIONS I AND II FOR $e > 1$

We now consider the orbits given by Eqs. (20), (29), and (36) for $e > 1$. The region covered by $\infty \geq e > 1$ and $\infty \geq s \geq 0$ is again divided into Regions I and II by a boundary curve s_1 given by Eq. (40) which extends from $s_1 = 0.25$ at $e = 1$ to $s_1 = 0$ at $e = \infty$ as $s_1 \rightarrow (\sqrt{27}e)^{-1}$ when $e \rightarrow \infty$. Just as for the case of $0 \leq e \leq 1$, Region I is the sector $0 \leq s \leq s_1$ and Region II is the sector $s_1 < s \leq \infty$. There is no Region II' because the s_2 curve from the sector $0 \leq e \leq 1$ never reaches the sector $e > 1$. Equation (20) describes the hyperbolic-type orbits in Region I, Eq. (29) describes the terminating orbits in Region I, and Eq. (36) describes the terminating orbits in Region II.

For the orbit described by Eq. (20) in Region I, we find that e_3 is less than $-1/12$ for $e > 1$, and q becomes infinite when the polar angle $\phi = \Psi_1$, where Ψ_1 is given by

$$sn^2(\gamma\Psi_1, k) = C,$$

where

$$C = -\frac{1/3 + 4e_3}{4(e_2 - e_3)},$$

and where γ and k are defined by Eqs. (21) and (22). As ϕ increases from Ψ_1 , $2K(k)/\gamma - \Psi_1$ is the next value of ϕ for q to become infinite. Thus Eq. (20) gives the hyperbolic-type orbit for $\Psi_1 \leq \phi \leq 2K(k)/\gamma - \Psi_1$ in Region I. The minimum distance q_{\min} of the planet from the star or black hole is given by Eq. (27) when the polar angle of the planet is given by $K(k)/\gamma$, where $dr/d\phi = 0$ at $q = q_{\min}$ (see a corresponding description given at the end of Sec. II). On the other hand, the planet intersects the horizontal axis at a distance q_h from the star or black hole, which can be obtained from Eq. (20) by setting the polar angle $\phi = \pi$. It is clear that q_h is not equal to q_{\min} generally except in the Newtonian limit.

The Newtonian limit corresponds to the case of very small s ($k^2 \simeq 0$). It can be shown that the equation for Ψ_1 becomes

$$\sin^2 \frac{\Psi_1}{2} = \frac{1}{2} - \frac{1}{2e},$$

from which we find

$$\Psi_1 = \cos^{-1} \left(\frac{1}{e} \right).$$

The approximate orbit Eqs. (14) and (13) for very small s and k^2 hold for $e \geq 1$ for which $E_0 \geq 0$ as well as for $0 \leq e < 1$ for which $E_0 < 0$. Thus, ignoring δ in Eq. (14), we get the Newtonian hyperbolic orbit given by

$$\frac{1}{r} = \frac{GM}{h^2} (1 - e \cos \phi),$$

where $\cos^{-1}(1/e) \leq \phi \leq 2\pi - \cos^{-1}(1/e)$ with $e > 1$, for which the minimum distance r_{\min} of the planet from the star equal to $h^2/[GM(1+e)]$ occurs at the polar angle $\phi = \pi$. The angle Ψ_1 ranges from 0 for $e = 1$ to $\pi/2$ for very large e .

For the special case of $k^2 = 1$ (where $s = s_1$) which is the boundary between Regions I and II, the angle Ψ_1 is given by

$$\tanh^2(\gamma\Psi_1) = \frac{2}{3} - \frac{1}{18}\sqrt{\frac{3}{g_2}},$$

where $g_2 = 1/12 - s_1^2$ and s_1^2 is given by Eq. (40), and γ by Eq. (44). The angle Ψ_1 for $k^2 = 1$ can range from 0 for $e = 1$ (parabolic-type orbit) to $2\tanh^{-1}(1/\sqrt{3}) = 1.31696 = 75.456^\circ$ for very large e . Because $K(1) = \infty$, the orbit equation given by Eq. (43) describes the trajectory of a planet that comes from infinity at an angle Ψ_1 to the horizontal axis and goes around the black hole located at the origin counter-clockwise as ϕ increases, and finally circles around the black hole with a radius that approaches q_{\min} given by Eq. (46). It can be called an asymptotic hyperbolic orbit.

Generally for $0 < k^2 < 1$, the angle Ψ_1 can range from 0 to 90° but the second angle $2K(k)/\gamma - \Psi_1$ at which ϕ becomes infinite can be an angle of any value because $\pi/2 < K(k) < \infty$, and thus the planet executing the hyperbolic-type orbit can go around the black hole many times as ϕ increases from Ψ_1 to $2K(k)/\gamma - \Psi_1$ before going off to infinity. We have seen a similar behavior for a parabolic-type orbit (see Fig. 4 a3–g3 and Fig. 8(a)) for which a planet comes from infinity at a polar angle $\phi = 0$, and can go around the black hole many times, before going off to infinity at a polar angle $\phi = 2K(k)/\gamma$.

A difference between the initial trajectories of a parabolic- and hyperbolic-type orbit may be noted as follows. For a parabolic-type orbit with the planet coming from infinity at the polar angle $\phi = 0$, it can be thought of as a limiting case of an elliptic-type orbit with $q_{\max} \rightarrow \infty$ on the horizontal axis, and thus the initial trajectory of the planet is perpendicular to the line joining it to the black hole at the origin. For a hyperbolic-type orbit, the initial trajectory of the planet coming from infinity is along a line that makes an angle $\Psi_1 > 0$ with the horizontal axis.

Region I also allows terminating orbits given by Eq. (29) for which the planet starts from $\phi = 0$ at a distance q_1 from the black hole given by Eq. (30) [with an initial trajectory perpendicular to the line joining the planet to the black hole] and terminates at the black hole with an angle $\phi_1 = K(k)/\gamma$.

Region II allows only terminating orbits given by Eq. (36). We find that a is less than $-1/12$ and that $q = \infty$ when the polar angle $\phi = \Psi_2$, where Ψ_2 is given by

$$cn(2\gamma\Psi_2, k) = \frac{1-D}{1+D},$$

where

$$D = -\frac{1}{\gamma^2}\left(\frac{1}{12} + a\right),$$

and where γ and k are given by Eqs. (34) and (35). The planet comes from infinity at a polar angle $\phi = \Psi_2$, and as ϕ increases, the orbit terminates at the black hole at a polar angle $\phi_2 = K(k)/\gamma$. As $s \rightarrow \infty$, we find from Eqs. (32)–(35) that $k^2 \rightarrow (2 + \sqrt{3})/4 = 0.933012702$, and from the equations for Ψ_2 and ϕ_2 that $\Psi_2 \rightarrow 0$ and $\phi_2 \rightarrow 0$, and thus the trajectory approaches that of a purely radial trajectory along a path that is very close to the horizontal axis.

A more detailed description and tabulation of all the orbits for $e > 1$ in Regions I and II similar to those we give for $0 \leq e \leq 1$ will be presented in a future publication.

The orbit Eqs. (20), (29), and (36), and the description of the orbits and the three regions where these orbit equations apply in Regions I, II, and II' for $0 \leq e \leq \infty$, and $0 \leq s \leq \infty$, complete our characterization of all possible planetary orbits in the Schwarzschild geometry.

We now briefly discuss how all this may be used for the Kerr geometry when the spinning black hole has a spin angular momentum per unit mass of the black hole that is relatively small compared to the orbital angular momentum per unit mass of the planet.

VI. KERR GEOMETRY

The spinning black hole is assumed to have a spin angular momentum J given by [1]

$$J = Mac, \quad (65)$$

where ac can be identified as the spin angular momentum per unit mass of the black hole and is the quantity to be compared with h , the orbital angular momentum per unit mass of the planet. Considering the Kerr geometry only in the equatorial plane, it becomes the Schwarzschild geometry in the limit $ac/h \rightarrow 0$.

The worldline of a particle moving in the equatorial plane $\theta = \pi/2$ satisfies the equations [1]

$$\dot{t} = \frac{1}{D} \left[\left(r^2 + a^2 + \frac{\alpha a^2}{r} \right) \kappa - \frac{\alpha ah}{cr} \right], \quad (66)$$

$$\dot{\phi} = \frac{1}{D} \left[\frac{\alpha ac \kappa}{r} + \left(1 - \frac{\alpha}{r} \right) h \right], \quad (67)$$

where $D \equiv r^2 - \alpha r + a^2$. For the equatorial trajectories of the planet in the Kerr geometry, the combined energy equation is

$$\begin{aligned} \dot{r}^2 + \frac{h^2 - a^2 c^2 (\kappa^2 - 1)}{r^2} - \frac{\alpha (h - ac \kappa)^2}{r^3} - \frac{c^2 \alpha}{r} \\ = c^2 (\kappa^2 - 1). \end{aligned} \quad (68)$$

Provided that $a^2/\alpha^2 < 1$ and $ac\kappa/h \ll 1$, to the first order in $ac\kappa/h$, it is not difficult to see, by comparing

Eqs. (66)–(68) with Eqs. (3)–(6), that we can rescale α to $\alpha' = \alpha(1 - 2ac\kappa/h)$, s to $s' = s(1 - ac\kappa/h)$, and ϕ to $\phi' = \phi[1 - b(ac\kappa/h)]$, where b is some approximation constant, such that the results we have presented for the orbits in the Schwarzschild geometry are approximately applicable for the orbits in the Kerr geometry in terms of the scaled parameters. That is, the orbits in the equatorial plane and their characterization for the Schwarzschild and Kerr geometries are qualitatively very similar to the first order in $ac\kappa/h$ except that the basic parameters s , α and ϕ have to be slightly rescaled. Again, we emphasize that the analogy is restricted to the Kerr geometry in the equatorial plane. Levin and Perez-Giz [5] obtained their orbits in the Kerr geometry from numerically integrating Eqs. (66)–(68) and it would be interesting to study and examine when and how the planet's orbits in the Kerr geometry that they obtained can be related with our results with the scaled parameters, and when and how they begin to differ significantly from those in the Schwarzschild geometry that we presented in this paper.

VII. TRAJECTORY OF LIGHT

We now consider the deflection of light by a gravitational field. We cannot use the proper time τ as a parameter. So we use some affine parameter σ along the geodesic [1]. Considering motion in the equatorial plane, the geodesic equations give Eqs. (3) and (5), and we replace the r -equation (4) by the first integral of the null geodesic equation, and we have [1]

$$\left(1 - \frac{\alpha}{r}\right)\dot{t} = \kappa, \quad (69)$$

$$c^2\left(1 - \frac{\alpha}{r}\right)\dot{t}^2 - \left(1 - \frac{\alpha}{r}\right)^{-1}\dot{r}^2 - r^2\dot{\phi}^2 = 0, \quad (70)$$

$$r^2\dot{\phi} = h, \quad (71)$$

where the derivative $\dot{}$ represents $d/d\sigma$. Substituting Eqs. (69) and (71) into (70) gives the combined energy equation

$$\dot{r}^2 + \frac{h^2}{r^2}\left(1 - \frac{\alpha}{r}\right) = c^2\kappa^2. \quad (72)$$

Substituting $dr/d\sigma = (dr/d\phi)(d\phi/d\sigma) = (h/r^2) \times (dr/d\phi)$ and $u = 1/r$ into the combined energy equation gives the differential equation for the trajectories of light in the presence of a gravitational field

$$\left(\frac{du}{d\phi}\right)^2 = \alpha u^3 - u^2 + \frac{c^2\kappa^2}{h^2}. \quad (73)$$

The constants κ and h have a physical significance through their ratio κ/h as follows: Let R denote the distance of the light beam to the center of a star or black hole when the trajectory of the light beam is such that $du/d\phi =$

0. R can either be associated with the distance of closest approach of the light beam to the black hole or with the initial distance to the black hole of the light beam. The latter case is associated with light trajectories that terminate at the black hole. With R so defined and letting $u_1 \equiv 1/R$, we can set $c^2\kappa^2/h^2$ to be equal to $u_1^2 - \alpha u_1^3$ [8].

It is again convenient to consider the problem in terms of the dimensionless inverse distance U defined by

$$U = \frac{\alpha}{r} = \alpha u = \frac{1}{q}. \quad (74)$$

U defined here is slightly different from the U defined by Eqs. (8) and (19) previously. In terms of U of Eq. (74), Eq. (73) becomes

$$\left(\frac{dU}{d\phi}\right)^2 = U^3 - U^2 + \frac{c^2\kappa^2\alpha^2}{h^2}. \quad (75)$$

Since $dU/d\phi = 0$ at $r = R$, one root U , which we call

$$U_1 \equiv \frac{\alpha}{R} \equiv \alpha u_1 \quad (76)$$

of the cubic equation $U^3 - U^2 + c^2\kappa^2\alpha^2/h^2 = 0$ is known, and the term $c^2\kappa^2\alpha^2/h^2$ on the right-hand side of Eq. (75) can be replaced by $-U_1^3 + U_1^2$, and the other two roots of the cubic equation $U^3 - U^2 - U_1^3 + U_1^2 = 0$ can be found from solving a quadratic equation. We denote the three roots of the cubic equation by e_1, e_2, e_3 . Thus, writing Eq. (75) as

$$\left(\frac{dU}{d\phi}\right)^2 = U^3 - U^2 - U_1^3 + U_1^2, \quad (77)$$

the trajectory of light represented by an equation for U as a function of the polar angle ϕ obtained from integrating Eq. (77) can be characterized by a single parameter U_1 , which essentially specifies either the distance of the closest approach or the initial distance of the light beam to the black hole. (These distances are scaled by the Schwarzschild radius of the black hole.) As in our discussion of the planets, our references to the initial position of the light beam assume that the trajectory of the light beam at that initial position is perpendicular to the line joining that position to the star or black hole. The range of U_1 is clearly between 0 and ∞ , where $U_1 = 0$ means that the light beam is infinitely far away from the black hole, $U_1 = 1$ means that the light beam is at the Schwarzschild radius at its closest approach or its initial position, and $U_1 = \infty$ means that the light beam is at the center of the black hole. As we show in the following, the region $0 \leq U_1 \leq \infty$ can be appropriately divided into three sectors which we again call Regions I, II, and II'. The similarity between the characterization of these three regions with that for the planetary orbits discussed in the previous sections will become apparent. Not surprisingly perhaps, only a single parameter which we choose to be U_1 , is needed for the characterization of the trajectories of a light beam in con-

trast to the two parameters (which we choose to be e and s), which we needed for the characterization of the orbits of a planet. The relationship between U_1 and R , from Eqs. (76) and (2), is

$$R = \frac{2}{U_1} \left(\frac{GM}{c^2} \right).$$

Region I: $0 \leq U_1 \leq 2/3$, or $\infty > R \geq 3GM/c^2$

Here, R denotes the distance of closest approach of a light beam that comes from a great distance. We let

$$e_1 = \frac{1}{2}[1 - U_1 + (1 + 2U_1 - 3U_1^2)^{1/2}], \quad e_2 = U_1, \\ e_3 = \frac{1}{2}[1 - U_1 - (1 + 2U_1 - 3U_1^2)^{1/2}], \quad (78)$$

with $e_1 > e_2 > e_3$, and we consider the region $e_1 > e_2 > U \geq e_3$, and write Eq. (77) as

$$\left(\frac{dU}{d\phi} \right)^2 = (e_1 - U)(e_2 - U)(U - e_3). \quad (79)$$

Equation (79) can be integrated [7] with ϕ expressed in terms of an inverse sn function. After a little algebra and re-arrangement, we find the trajectory's equation in terms of the Jacobian elliptic functions of modulus k to be

$$\frac{1}{q} = \frac{(e_1 - e_3)e_2 - (e_2 - e_3)e_1 sn^2(\gamma\phi, k)}{(e_1 - e_3) - (e_2 - e_3)sn^2(\gamma\phi, k)}, \quad (80)$$

where

$$\gamma = \frac{(e_1 - e_3)^{1/2}}{2}, \quad k^2 = \frac{e_2 - e_3}{e_1 - e_3}. \quad (81)$$

The angle of deflection $\Delta\phi$ can be obtained as follows: If we set $q = \infty$ and also set $\phi = \pi/2 + \Delta\phi/2$ as the incoming angle in Eq. (80) [see Fig. 9(a) for the special case of $\Delta\phi/2 = 45^\circ$], where $\Delta\phi$ denotes the total angle of deflection of light by the mass M , we get the following equation for determining $\Delta\phi$ exactly:

$$sn^2 \left[\gamma \left(\frac{\pi}{2} + \frac{\Delta\phi}{2} \right), k \right] = \frac{(e_1 - e_3)e_2}{(e_2 - e_3)e_1},$$

where e_1, e_2, e_3, γ, k , are given by Eqs. (78) and (81). It can also be expressed as

$$\Delta\phi = -\pi + \frac{2}{\gamma} sn^{-1}(\psi, k), \quad (82)$$

where

$$\psi = \left[\frac{(e_1 - e_3)e_2}{(e_2 - e_3)e_1} \right]^{1/2}.$$

Equations (80)–(82) were first given by one of us in Ref. [6]. Examples of these trajectories obtained from Eq. (80) are presented in polar coordinates (q, ϕ) in Fig. 9, where the black hole is located at the origin. By setting the angles of deflection $\Delta\phi$ presented in Fig. 9 to be $\pi/2, \pi, 3\pi/2, 2\pi$, the corresponding values of U_1 can be

determined from Eqs. (82) and (78) using the MAPLE FSOLVE program, and they are found to correspond to the distances of closest approach $R = 4.6596GM/c^2, 3.5206GM/c^2, 3.2085GM/c^2, 3.0902GM/c^2$, respectively. The case of $R = 3.5206GM/c^2$ is interesting as it corresponds to the light ray being turned around by 180° ,

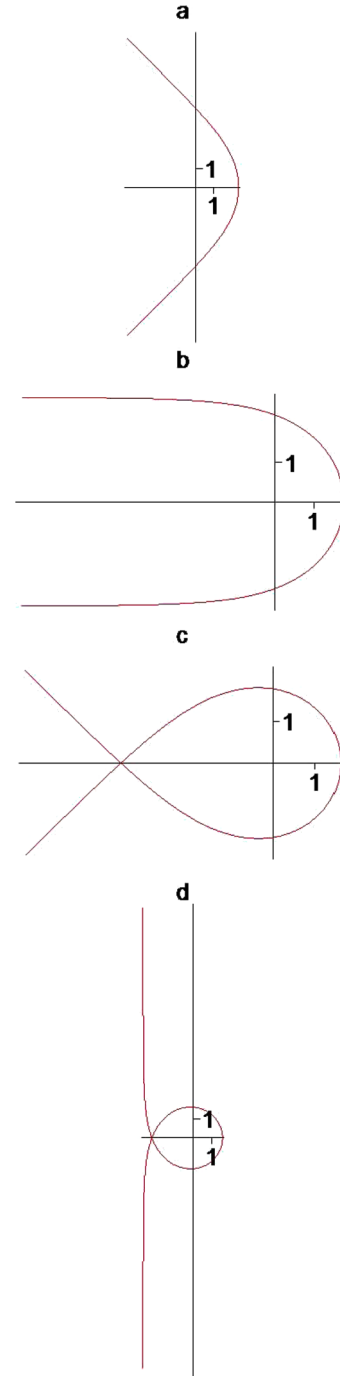


FIG. 9 (color online). Trajectories of light (with Schwarzschild radius marked on axes) for (a) $U_1 = 0.42922$, $\Delta\phi = \pi/2$. (b) $U_1 = 0.56808$, $\Delta\phi = \pi$. (c) $U_1 = 0.62334$, $\Delta\phi = 3\pi/2$. (d) $U_1 = 0.64720$, $\Delta\phi = 2\pi$.

which is called retro-lensing [9]. That the upper boundary of Region I characterized by $U_1 = 2/3$ or $R = 3GM/c^2$ is a very special case can be seen mathematically because it results in $e_1 = e_2 = 2/3$, $e_3 = -1/3$, and hence $k^2 = 1$, $\gamma = 1/2$ and $U = 2/3 = \text{const}$ from Eqs. (81) and (80). Physically, it results in the light circling the black hole with a radius $R = 3GM/c^2$ even though the trajectory has been shown to be an unstable one [1]. This known result can also be simply obtained from the equation of motion $d^2U/d\phi^2 = (3/2)U^2 - U$ for $U = \text{const}$ and thus $U = 2/3$. If one compares the size of the unstable circular photon orbit with the allowed limiting radii of the planetary asymptotic periodic orbits ($2 \leq q_{\min} \leq 2.25$ or $4GM/c^2 \leq r_{\min} \leq 4.5GM/c^2$), one can see that the radius of the asymptotic circular path of a planet around a black hole is still a little larger than that for a photon, but not by much.

The lower boundary of Region I characterized by $U_1 = 0$ or $R = \infty$ gives $e_1 = 1$, $e_2 = e_3 = 0$, $k^2 = 0$ and $\gamma = 1/2$, and thus gives $U = 0$ or $r = \infty$, which is a limiting case as the light ray that is infinitely far away at its closest approach to the black hole is completely undeflected.

As in the case of the Region I particle orbits discussed in Sec. III, the squared modulus k^2 of the elliptic functions that describe the trajectories of light here also covers the entire range $0 \leq k^2 \leq 1$; it varies from 0 at the lower boundary to 1 at the upper boundary.

For small U_1 , the trajectory of light given by Eq. (80) has been shown [6] to reduce to

$$\frac{1}{r} \simeq \frac{\cos\phi}{R} + \frac{GM}{c^2 R^2} (1 + \cos\phi + \sin^2\phi), \quad (83)$$

and the total deflection of light to reduce to the well-known result

$$\Delta\phi \simeq \frac{4GM}{c^2 R}. \quad (84)$$

It can be shown from our exact result given by Eq. (82) that this approximate expression (84) still gives an accuracy of two significant figures for $U_1 = 0.1$ or $R = 20GM/c^2$.

As U_1 approaches $2/3$, or as R approaches $3GM/c^2$, we may let $U_1 = 2/3 - \delta$, where $\delta \equiv (2/3)(1 - 3GM/c^2 R)$ is a small positive number. From Eqs. (78) and (81), we can express the quantities $2/\gamma$, ψ and k appearing in Eq. (82) in power series in δ and find, to the first order in δ , $2/\gamma \simeq 4(1 - \delta/2 + \dots)$, $\psi \simeq 1 - \delta/2 + \dots$, and $k \simeq 1 - \delta + \dots$. Substituting these into Eq. (82) immediately gives an expression for $\Delta\phi$ which is correct to the first order in δ . If an attempt is made to find an expansion of $sn^{-1}(\psi, k)$ near $k = 1$, since $sn^{-1}(\psi, 1) = \tanh^{-1}\psi = \ln[(1 + \psi)/(1 - \psi)]^{1/2}$, the expansion would involve terms in $\ln\delta$ (which is a large number for small δ) and ordering the expansion terms in the right way can be tricky. Different forms of such expansions have been given and

studied by various authors [10]. As we showed above and in Fig. 9, our exact expressions given by Eqs. (80) and (82) can be used simply and directly for all cases in Region I.

As U_1 increases beyond $2/3$ or as the distance of closest approach R of the light beam to the black hole becomes smaller than $3GM/c^2$, the light is not just deflected but is absorbed by and terminates at the black hole. It is useful to divide the region $2/3 < U_1 \leq \infty$ or $3GM/c^2 > R \geq 0$ into two regions that we call Regions II and II' that are separated by the Schwarzschild horizon, as we discuss below. Region II is for R from $3GM/c^2$ up to the Schwarzschild horizon, and Region II' is for R from the Schwarzschild horizon up to the center of the black hole.

Region II: $2/3 < U_1 \leq 1$, or $3GM/c^2 > R \geq 2GM/c^2$

Here, R denotes the initial distance to the black hole of the light beam which has initial trajectory (as ϕ increases from 0) perpendicular to the line joining it to the black hole.

As U_1 increases beyond $2/3$, U_1 becomes greater than $[1 - U_1 + (1 + 2U_1 - 3U_1^2)^{1/2}]/2$, and the order of the three roots must be changed to maintain the inequality $e_1 > e_2 > e_3$. We write

$$\begin{aligned} e_1 &= U_1, & e_2 &= \frac{1}{2}[1 - U_1 + (1 + 2U_1 - 3U_1^2)^{1/2}], \\ e_3 &= \frac{1}{2}[1 - U_1 - (1 + 2U_1 - 3U_1^2)^{1/2}]. \end{aligned} \quad (85)$$

We consider the region $U > e_1 > e_2 > e_3$, and write Eq. (77) as

$$\left(\frac{dU}{d\phi}\right)^2 = (U - e_1)(U - e_2)(U - e_3). \quad (86)$$

Equation (86) can be integrated [7] with ϕ expressed in terms of an inverse sn function. After some rearrangement, we find

$$\frac{1}{q} = \frac{e_1 - e_2 sn^2(\gamma\phi, k)}{cn^2(\gamma\phi, k)}, \quad (87)$$

where γ and k^2 are calculated using the same expressions given by Eq. (81) but with e_1, e_2, e_3 given by Eq. (85).

The expressions for e_1, e_2, e_3 given by Eqs. (78) and (85) coincide at $k^2 = 1$ for which $e_1 = e_2 = 2/3$, $e_3 = -1/3$, and both Eqs. (80) and (87) give $U = 2/3$ or $r = 3GM/c^2$ independent of ϕ .

Equation (87) gives a trajectory of light which terminates at the black hole when $\phi = \phi_2 = K(k)/\gamma$. As in our discussion of the terminating orbits for the planet, the terminating light ray trajectories can be characterized by the angle ϕ_2 with which the light beam enters the center of the black hole.

As U_1 increases from $2/3$ to 1, k^2 covers the entire range $1 \geq k^2 \geq 0$; it decreases from 1 to 0. When $U_1 = 1$, i.e. when the light beam grazes the Schwarzschild horizon, $e_1 = 1$, $e_2 = e_3 = 0$, $k^2 = 0$, $\gamma = 1/2$, and we have the trajectory of light given by

$$\frac{1}{q} = \frac{1}{\cos^2(\phi/2)}, \quad (88)$$

which gives, for $\phi = 0$, $U = 1$ or $r = \alpha$, and for $\phi = \pi$, $U = \infty$ or $r = 0$, i.e. the light is absorbed at the center of the black hole. Examples of the trajectories of light obtained from Eqs. (87) and (88) for $U_1 = 5/6 = 0.83333$ ($R = 2.4GM/c^2$) and 1 ($R = 2GM/c^2$) in Region II are shown as the solid lines in Fig. 10(a) and 10(b). The path that emerges from the center of the black hole when ϕ is continued beyond ϕ_2 (shown as a dotted line in Fig. 10) again may be interesting if the concept of white hole is of any physical relevance.

When the distance R to the black hole at $\phi = 0$ is inside the Schwarzschild horizon, the terminating path takes on a somewhat different form as we show below.

Region II': $1 < U_1 \leq \infty$, or $2GM/c^2 > R \geq 0$

Here, R has the same meaning as that in Region II. As U_1 increases beyond 1, i.e. when R is less than the Schwarzschild radius, e_1 in Eq. (85) remains real, while e_2 and e_3 become complex. We now write the three roots of the cubic equation $U^3 - U^2 - U_1^3 + U_1^2 = 0$ as a , b , and \bar{b} given by

$$a = U_1, \quad b = \frac{1}{2}[1 - U_1 + i(3U_1^2 - 2U_1 - 1)^{1/2}], \\ \bar{b} = \frac{1}{2}[1 - U_1 - i(3U_1^2 - 2U_1 - 1)^{1/2}]. \quad (89)$$

We consider the region $U > a$, and write Eq. (77) as

$$\left(\frac{dU}{d\phi}\right)^2 = (U - a)(U - b)(U - \bar{b}). \quad (90)$$

This equation can be integrated [7] with ϕ expressed in terms of an inverse cn function. After a little algebra, we find

$$\frac{1}{q} = a + \gamma^2 \frac{1 - cn(\gamma\phi, k)}{1 + cn(\gamma\phi, k)} \\ = a + \gamma^2 \frac{tn^2(\gamma\phi, k) dn^2(\gamma\phi, k)}{1 + cn(\gamma\phi, k)}, \quad (91)$$

where

$$\gamma = [U_1(3U_1 - 2)]^{1/4} \quad (92)$$

and

$$k^2 = \frac{1}{2} - \frac{3U_1 - 1}{4\sqrt{U_1(3U_1 - 2)}} = \frac{1}{2} - \frac{3a - 1}{4\gamma^2}. \quad (93)$$

Equation (91) gives the trajectory of light when R is inside the Schwarzschild horizon and it terminates at the black hole when $\phi = \phi_2 = 2K(k)/\gamma$, where k and γ are given by Eqs. (93) and (92). On the boundary with Region II where $U_1 = 1$, and $k^2 = 0$, $\gamma = 1$ from Eqs (93) and (92), Eq. (91) becomes Eq. (88) and thus there is no discontinuity in the orbit as it makes a transition from Region II to Region II' across $U_1 = 1$.

We note that as in the case of Region II' for the planetary orbits, Region II' for light trajectories covers a semi-

infinite range of the parameter characterizing it ($1 < U_1 \leq \infty$) but is of relevance only to a very small physical region $2GM/c^2 > R \geq 0$ for the initial position of a light beam inside the Schwarzschild horizon. The terminating orbits of light rays in Region II' are also of very little variety as ϕ_2 is restricted to a limited range of $0 \leq \phi_2 \leq \pi$. An example of a terminating trajectory obtained from Eq. (91) is shown as the solid line in Fig. 10(c) for $U_1 = 10$ ($R = 0.2GM/c^2$); the dotted line again represents a trajectory of light coming out from the center of the black hole as ϕ is continued beyond ϕ_2 . It may be of some mathematical interest to note that as $U_1 \rightarrow \infty$ or $R \rightarrow 0$, the squared modulus of the Jacobian elliptic functions used to describe the trajectories k^2 approaches a value $(2 - \sqrt{3})/4 = 0.0669873$ that is the same as that given in Sec. IV for the case of Region II' for the planetary orbits. Thus, the

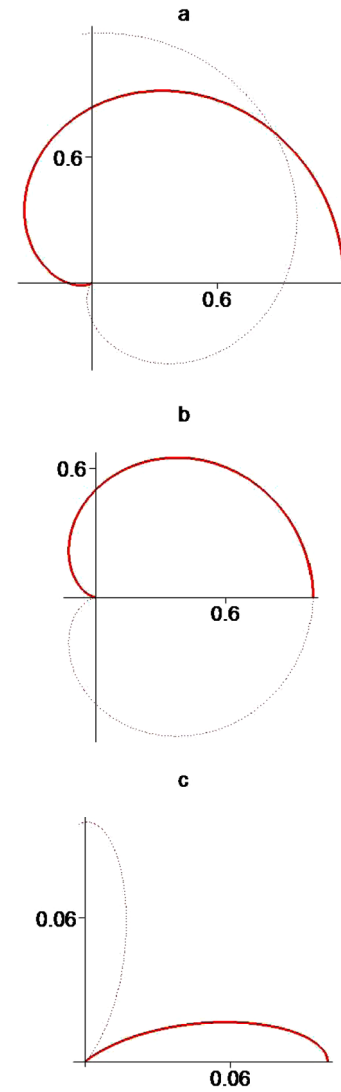


FIG. 10 (color online). Trajectories of light that terminated (dotted line represents trajectory beyond $r = 0$) (a) $U_1 = 0.8333$, $\phi_1 = 3.8345$. (b) $U_1 = 1$, $\phi_1 = \pi$. (c) $U_1 = 10$, $\phi_1 = 0.78133$.

squared modulus of the elliptic functions that describe the terminating light trajectories in Region II' is restricted to a very small range $0 < k^2 \leq 0.0669873$ even as Region II' consists of a very large interval $1 < U_1 \leq \infty$.

VIII. SUMMARY

We have presented exact analytic expressions given by Eqs. (20), (29), and (36) for the planetary orbits in the Schwarzschild geometry. The equations relate the distance r of the planet from the star or black hole to the polar angle ϕ and are described explicitly by Jacobian elliptic functions of modulus k . Equation (20) gives a nonterminating orbit that can be referred to as an elliptic, parabolic or hyperbolic-type, including an asymptotic one, while Eqs. (29) and (36) give terminating orbits that describe a planet plunging into the center of a black hole. One of the most important aspects of our analysis is the construction of a map with coordinates (e, s) that we use to view all possible orbits in their entirety, where the two dimensionless parameters e and s are defined by Eqs. (11) and (12) which we call the energy and field parameters, respectively. For $0 \leq e \leq \infty$, we show that there are three regions which we call Regions I ($0 \leq s \leq s_1$), II ($s_1 < s \leq s_2$) and II' ($s_2 < s \leq \infty$) where these orbits are applicable, and where s_1 and s_2 that depend on e are given by Eqs. (40) and (57), respectively, (Fig. 2). For $0 \leq e \leq 1$, Region I has periodic (elliptic-type) and unbounded (parabolic-type) orbits given by Eq. (20) and terminating orbits given by Eq. (29), while Regions II and II' have terminating orbits only given by Eq. (36). We have divided Region I into grids that consist of lines of constant precession angle $0 \leq \Delta\phi \leq \infty$ given by Eq. (25) and lines of constant true eccentricity $0 \leq \varepsilon \leq 1$ defined by Eq. (28) [Fig. 3]; the lines of constant $\Delta\phi$ are obtained from solving Eqs. (38) and (A6), and those of constant ε from solving Eqs. (38) and (B1). These grids make the identification of all possible periodic orbits convenient and precise. Numerous numerical results for orbits in Region I are presented in Tables I, II, III, IV, V, and VI, and examples of precessing orbits, including the unbounded ones, are shown in Figs. 4 and 5. Among the interesting results, for example, Table VI for $\Delta\phi = 2\pi$, $e = 1$, $s = 0.248804$ and Fig. 4 f3 show that a planet coming from infinity at zero polar angle, makes a complete loop about the black hole, and returns to infinity with a polar angle that approaches 2π . Figure 3, or a more refined version of it that can be constructed using the expressions for $\Delta\phi$ and ε that we presented, can be fruitfully used with the experimental observation data. The terminating orbits of Region I and those of Region II' require the planet to be initially very close to the black hole or within the Schwarzschild horizon. The terminating orbits of Region II, on the other hand, are more interesting as the planet can be initially at a distance $1 < q_2 \leq \infty$. We have shown how the periodic orbits of Region I become the asymptotic periodic orbits as $s \rightarrow s_1$, and then become

terminating orbits as s becomes greater than s_1 . For $e > 1$, we have Region I ($0 \leq s \leq s_1$) where there are hyperbolic-type orbits given by Eq. (20) and terminating orbits given by Eq. (29), and Region II ($s_1 < s \leq \infty$) where there are only terminating orbits given by Eq. (36).

We have also presented exact analytic expressions given by Eqs. (80), (87), and (91) for the trajectories of light in the presence of a star or black hole depending on the value of one parameter U_1 that has a range which can be divided into three regions: Regions I ($0 \leq U_1 \leq 2/3$), II ($2/3 < U_1 \leq 1$) and II' ($1 < U_1 \leq \infty$), where U_1 is defined by Eq. (76). In Region I, the deflection of light can range from small angles to going continuously around the star or black hole in a circle. In Regions II and II', light is absorbed into the center of the black hole. Among the interesting results, a deflection of light by 180° requires a distance of closest approach R to the black hole equal to $3.5206GM/c^2$ [Fig. 9(b)], and for $R < 3GM/c^2$, light will be absorbed by the black hole.

We have thus presented a complete map that can help to identify characteristics of stars and black holes (that are not spinning too fast) from the observed characteristics of objects or light beams that are affected by them.

ACKNOWLEDGMENTS

We are very grateful to an anonymous referee whose very constructive comments help to clarify and improve the content of this manuscript.

APPENDIX A: RELATION AMONG s , e AND k^2

In this Appendix, we derive the relation among s , e and k^2 given by Eqs. (38) and (39). Substituting Eq. (23) into Eq. (22) and after a little algebra, we find

$$\tan\frac{\theta}{3} = \frac{\sqrt{3}k^2}{2 - k^2}, \quad (\text{A1})$$

and hence we find

$$\sin\frac{\theta}{3} = \frac{\sqrt{3}k^2}{2\sqrt{1 - k^2 + k^4}}, \quad (\text{A2})$$

$$\cos\frac{\theta}{3} = \frac{2 - k^2}{2\sqrt{1 - k^2 + k^4}}. \quad (\text{A3})$$

We then find

$$\begin{aligned} \cos\left(\frac{\theta}{3} + \frac{4\pi}{3}\right) &= \frac{-1 + 2k^2}{2\sqrt{1 - k^2 + k^4}}, \\ \cos\left(\frac{\theta}{3} + \frac{2\pi}{3}\right) &= \frac{-1 - k^2}{2\sqrt{1 - k^2 + k^4}}. \end{aligned} \quad (\text{A4})$$

Equations (A3)–(A5) and (23) allow e_1 , e_2 , e_3 to be expressed in terms of g_2 and k^2 as

$$e_1 = \sqrt{\frac{g_2}{12} \frac{2 - k^2}{\sqrt{1 - k^2 + k^4}}}, \quad e_2 = \sqrt{\frac{g_2}{12} \frac{-1 + 2k^2}{\sqrt{1 - k^2 + k^4}}},$$

$$e_3 = \sqrt{\frac{g_2}{12} \frac{-1 - k^2}{\sqrt{1 - k^2 + k^4}}}. \quad (\text{A5})$$

Substituting Eq. (A3) into the relation $\cos\theta = -3\cos(\theta/3) + 4\cos^3(\theta/3)$, and substituting the result into Eq. (24) gives the relation among s , e and k^2 given by Eqs. (38) and (39). For $k^2 = 1$, we get $\cos\theta = -1$ from Eqs. (38) and (39), and from Eq. (A5) we get $e_1 = e_2 = \sqrt{g_2/12} = -(1/2)e_3$.

From Eqs. (25), (21), (A5), and (10), we find an expression for the precession angle $\Delta\phi$ given by Eq. (25) in terms of k and s to be

$$\Delta\phi = 4K(k) \left(\frac{1 - k^2 + k^4}{1 - 12s^2} \right)^{1/4} - 2\pi. \quad (\text{A6})$$

APPENDIX B: THE ENERGY PARAMETER e AND THE TRUE ECCENTRICITY ε IN REGION I

In this Appendix, we show the relation between the energy parameter e and the true eccentricity ε . The energy parameter e in all three Regions I, II, and II' is defined by Eq. (11). The general or true eccentricity ε is defined by Eq. (28). From Eq. (28), (26), and (27) and using the expressions (A5) of e_1 , e_2 , e_3 in terms of k^2 given in Appendix A, we find that ε can be expressed as

$$\varepsilon = \frac{6(e_2 - e_3)}{1 + 6(e_2 + e_3)}$$

or

$$\varepsilon = \frac{3k^2\sqrt{1 - 12s^2}}{2\sqrt{1 - k^2 + k^4} - (2 - k^2)\sqrt{1 - 12s^2}}. \quad (\text{B1})$$

For small s^2 and k^2 , we find that

$$\varepsilon \simeq \frac{3k^2/2}{1 - (1 - 6s^2)} \simeq \frac{k^2}{4s^2} \simeq e \quad (\text{B2})$$

because $k^2 \simeq 4es^2$ for very small k^2 and s^2 [6]. We thus confirm the identification of e defined in Eq. (11) with the eccentricity of the orbit in Newtonian mechanics. As we pointed out in the text, ε is generally not equal to e . However, as we show below, $\varepsilon = e$ exactly when $e = 1$ and in this case the orbits are unbounded.

For the possibility of unbounded orbits in Region I, we set the initial $q = \infty$ at $\phi = 0$ in Eq. (20), and get

$$\frac{1}{3} + 4e_3 = 0, \quad (\text{B3})$$

or

$$e_3 = -\frac{1}{12}. \quad (\text{B4})$$

Using Eqs. (23), (10), and (A4) that give e_3 in terms of s and k^2 , and after a little algebra, we find the simple

equation that relates s to k^2 on $e = 1$ to be given by Eq. (51).

This simple Eq. (51) between s and k^2 for $e = 1$ can be used for any $0 \leq k^2 \leq 1$. For example, we find that for $k^2 = 1$, $s = 1/4 = 0.25$, and for $k^2 = 1/2$, $s = 1/(3\sqrt{2}) = 0.235702$. For $e = 1$, and for small k^2 , we have $s^2 \simeq k^2/4$ which is a special case of $k^2 \simeq 4es^2$ that is valid more generally for $0 \leq e \leq 1$.

In addition, we find $g_2 = 1/12 - s^2 = 1/12 - k^2/[4(1 + k^2)^2]$ and therefore

$$g_2 = \frac{1 - k^2 + k^4}{12(1 + k^2)^2}, \quad (\text{B5})$$

and from the expression for e_1 and e_2 given by Eq. (A5), we find

$$e_1 = \frac{2 - k^2}{12(1 + k^2)}, \quad e_2 = \frac{-1 + 2k^2}{12(1 + k^2)}. \quad (\text{B6})$$

Thus, from the expressions (27), (30), and (21) for q_{\min} , q_1 , and γ , we find that when $e = 1$, they have the simple expressions given by Eqs. (53), (54), and (52).

Also, substituting Eq. (48) into Eq. (B1) shows that $\varepsilon = 1$ when $e = 1$, i.e. ε and e coincide at $e = 1$.

APPENDIX C: SOME SIMPLE RELATIONS FOR THE SPECIAL CASE OF $k^2 = 1/2$

It is known that in elliptic functions, the squared modulus $k^2 = 1/2$ is a special value for which many simple relations arise. We first consider the case of $k^2 = 1/2$ in Region I. We note that substituting $k^2 = 1/2$ into Eq. (22) gives a relation $e_1 + e_3 = 2e_2$, and substituting the expressions of e_1 , e_2 , e_3 from Eq. (23) into this relation gives $\theta/3 = \pi/6$, or $\theta = \pi/2$. Thus, $\cos\theta = 0$, which results in

$$g_3 = 0 \quad (\text{C1})$$

from Eq. (24), which in turn gives a simple relationship

$$s^2 = \frac{1}{6(1 - e^2)} \left(1 - \sqrt{\frac{1 + 2e^2}{3}} \right). \quad (\text{C2})$$

For example, we have $s = \sqrt{(3 - \sqrt{3})/18} = 0.265408$ for $e = 0$, and $s = 1/(3\sqrt{2}) = 0.235702$ for $e = 1$ (using L'Hospital rule). These two values represent the two terminal coordinates of the constant $k^2 = 1/2$ line in Region I (see Fig. 1). The other solution of Eq. (C1) is Eq. (58), which is applicable for Region II as we shall show later in this Appendix.

We also find from Eq. (23) that

$$e_1 = -e_3 = \frac{\sqrt{g_2}}{2}, \quad e_2 = 0, \quad (\text{C3})$$

and

$$\gamma = \sqrt[4]{g_2}. \quad (\text{C4})$$

and the orbit Eq. (20) becomes

$$\frac{1}{q} = \frac{1}{3} - 2\sqrt{g_2}cn^2(\gamma\phi, 1/\sqrt{2}),$$

where the s value for g_2 in this case is given by Eq. (C2) for Region I. The precession angle $\Delta\phi$ can be found from Eq. (25) and from $K(1/\sqrt{2}) = 1.85407$. It is given by

$$\frac{\Delta\phi}{\pi} = \frac{1.18034}{\sqrt[4]{g_2}} - 2.$$

From Eqs. (26)–(28) and (C3), we find

$$\varepsilon = \frac{6(e_2 - e_3)}{1 + 6(e_2 + e_3)} = \frac{3\sqrt{g_2}}{1 - 3\sqrt{g_2}}, \quad (\text{C5})$$

which can be inverted and solved for s in terms of ε , giving

$$s^2 = \frac{3 + 6\varepsilon - \varepsilon^2}{36(1 + \varepsilon)^2}. \quad (\text{C6})$$

Substituting Eq. (C6) into Eq. (C1) gives e in terms of ε as

$$e^2 = 1 - \frac{12(1 + \varepsilon)^2(1 - \varepsilon)(1 + 3\varepsilon)}{(3 + 6\varepsilon - \varepsilon^2)^2}. \quad (\text{C7})$$

Since for $e = 0$, $s = \sqrt{(3 - \sqrt{3})/18}$ when $k^2 = 1/2$ as we showed above, substituting this s value into Eq. (C1) gives $\varepsilon = (2/\sqrt{-3 + 2\sqrt{3}} - 1)^{-1} = 0.516588$. For $e = 1$, $s = 1/(3\sqrt{2})$ when $k^2 = 1/2$, and substituting this s value into Eq. (C1) gives $\varepsilon = 1$ as it should. Thus, Eqs. (C6) and (C7) are the parametric equations for the line of constant $k^2 = 1/2$, which can be used instead of Eq. (C2) as ε takes the values between 0.516588 and 1.

Also, substituting $e_2 = 0$ from Eq. (C3) into Eq. (27) gives

$$q_{\min} = 3 \quad (\text{C8})$$

independent of e for $k^2 = 1/2$, as shown in Table III.

We now consider $k^2 = 1/2$ in Region II. From Eqs. (35) and (33), we have

$$a = A + B = 0. \quad (\text{C9})$$

From Eq. (32), and from $A = -B$, and $A^3 = -B^3$, we arrive again at Eq. (C1) with the same g_3 given by Eq. (10). This explains why we stated after Eq. (C2) that the other solution of Eq. (C1) given by Eq. (58) gives the relation between s and e for Region II. The two Eqs. (C3) and (58) that give simple relations between s and e in two different regions and that arise as two different solutions of the same Eq. (C1) show a rather remarkable symmetry exhibited by the special case $k^2 = 1/2$.

It also follows from Eqs. (32) and (34) that

$$A = \frac{1}{2} \left(\frac{-g_2}{3} \right)^{1/2} = \frac{1}{12} \sqrt{12s^2 - 1}, \quad (\text{C10})$$

$$\gamma = (3A^2)^{1/4} = \frac{1}{2} [\frac{1}{3} (12s^2 - 1)]^{1/4}, \quad (\text{C11})$$

and that the orbit Eq. (36) becomes

$$\frac{1}{q} = \frac{1}{3} + 4\gamma^2 \frac{1 - cn(2\gamma\phi, 1/\sqrt{2})}{1 + cn(2\gamma\phi, 1/\sqrt{2})}, \quad (\text{C12})$$

where the s value for the above equations is given by Eq. (58) for $0 \leq e \leq 1$.

Since $a = 0$, the initial distance q_2 of the planet from the black hole is $q_2 = 3$ from Eq. (37), independent of e , as shown in Table X.

APPENDIX D: THE BOUNDARY OF REGION II

On the upper boundary $s_2^2 = 1/(1 - e^2)$ of Region II, the planet starts from the Schwarzschild horizon given by $q = 1$, which implies that for $\phi = 0$, $1/q = 1/3 + 4a$ from Eq. (36), or

$$1 = \frac{1}{3} + 4a. \quad (\text{D1})$$

Hence,

$$a = A + B = \frac{1}{6}. \quad (\text{D2})$$

Since from Eqs. (32) and (17),

$$AB = \frac{1}{4} \left(g_3^2 - \frac{\Delta}{27} \right)^{1/3} = \frac{g_2}{12}, \quad (\text{D3})$$

we can conclude from Eqs. (35) and (34) that k^2 and γ are given on the boundary $s_2^2 = 1/(1 - e^2)$ of Region II by Eqs. (60) and (61).

In particular, for $e = 0$, $s = 1$, we find $\gamma = (5/16)^{1/4} = 0.747674$, $k^2 = (1 - 1/\sqrt{5})/2 = 0.276393$, and this is the minimum value of k^2 in Region II.

We now consider the special case of $e = 1$ of Region II. Consider the unbounded orbit of a planet coming from infinity at $\phi = 0$ that requires, from Eq. (36), that

$$\frac{1}{3} + 4a = 0, \quad (\text{D4})$$

or

$$a = -\frac{1}{12}. \quad (\text{D5})$$

From

$$A + B = a = -\frac{1}{12}, \quad (\text{D6})$$

and

$$AB = \frac{g_2}{12}, \quad (\text{D7})$$

and from Eqs. (34) and (35), we find Eqs. (62) and (64) that give k^2 and γ in terms of s for $e = 1$ of Region II.

APPENDIX E

The special case of $g_3 = 0$ has been shown in Appendix C to correspond to the special case of $k^2 =$

$1/2$ that gives the curves given by Eqs. (C2) and (58) in Regions I and II. The case of $g_2 = 0$ or $s^2 = 1/12$ ($s = 1/2\sqrt{3} = 0.288675135$) in Region II is also interesting and significant. If g_2 of Eq. (10) is equal to zero, then $\Delta = 27g_3^2$ from Eq. (17), and from Eqs. (32)–(35), we find $A = (2g_3)^{1/3}/2$, $B = 0$, $a = A$, $\gamma = (3A^2)^{1/4}$, and noting that $A < 0$ for $s^2 = 1/12$ and $0 \leq e \leq \infty$, we have

$$k^2 = \frac{1}{2} - \frac{\sqrt{3}A}{4|A|} = \frac{1}{2} + \frac{\sqrt{3}}{4} = 0.933012702,$$

which is independent of e , i.e. the constant $k^2 = (2 + \sqrt{3})/4$ curve in Region II just above the boundary curve of Regions I and II in Fig. 2 is a horizontal line. Thus, the terminating orbits represented by Eq. (36) for any point along this horizontal line (i.e. for any $0 \leq e \leq \infty$, $s = 0.288675135$) are represented by elliptic functions of the

same squared modulus given above. The initial position of the planet still depends on e ; it is finite for $e < 1$ and is infinite for $e \geq 1$ (the initial trajectory of the planet is perpendicular to the line joining the planet to the black hole for $0 \leq e \leq 1$ but is at an angle Θ for $e > 1$ described in Sec. V).

If the cubic polynomial on the right-hand side of Eq. (9) is denoted by $f(U)$, requiring $f'(U) = f''(U) = 0$ gives $g_2 = 0$ which in turn gives $s = 1/2\sqrt{3}$. From the analysis of the “effective potential energy curves” that made use of a cubic polynomial equivalent to $f(U)$, this special value of $s = 1/2\sqrt{3}$ has been obtained and associated with the so-called innermost stable circular orbit of radius $q = 3$ [1]. As our analysis clearly identifies this value of s to be in Region II where all the orbits are terminating, we are unable to identify it with any stable circular orbit.

-
- [1] M. P. Hobson, G. Efstathiou, and A. N. Lasenby, *General Relativity: An Introduction for Physicists* (Cambridge University Press, New York, 2006), Chaps. 9 and 10.
- [2] E. T. Whittaker, *A Treatise on the Analytical Dynamics of Particles and Rigid Bodies* (Dover, New York, 1944), 4th ed., Chap. XV.
- [3] Y. Hagihara, *Jpn. J. Astron. Geophys.* **8**, 67 (1931).
- [4] S. Chandrasekhar, *The Mathematical Theory of Black Holes* (Oxford University Press, Oxford, 1983), Chap. 3.
- [5] J. Levin and G. Perez-Giz, *Phys. Rev. D* **77**, 103005 (2008).
- [6] F. T. Hioe, *Phys. Lett. A* **373**, 1506 (2009).
- [7] P. F. Byrd and M. D. Friedman, *Handbook of Elliptic Integrals for Engineers and Scientists* (Springer-Verlag, New York, 1971), 2nd ed.. See, in particular, pp. 72, 74, 81, 86 for the formulas used in this paper.
- [8] See e.g. J. L. Martin, *General Relativity: A Guide to its Consequences for Gravity and Cosmology* (Ellis Horwood Ltd., Chichester, England, 1988), Chap. 4.
- [9] See e.g. D. E. Holz and J. A. Wheeler, *Astrophys. J.* **578**, 330 (2002).
- [10] S. V. Iyer and A. O. Petters, *Gen. Relativ. Gravit.* **39**, 1563 (2007); C. R. Keeton and A. O. Petters, *Phys. Rev. D* **72**, 104006 (2005).